Nano Research

ISSN 1998-0124 CN 11-5974/O4
https://doi.org/10.26599/NR.2026.94908736

Review Article

Carbon dots@MOF composites: Synthetic strategies, luminescence regulation, and emerging applications

Boyang Wang[1], Nina Qian[1](✉), Siyu Lu[2](✉)

[1] Anhui Provincial Key Laboratory of Advanced Catalysis and Energy Materials, Anhui Key Laboratory of Optoelectronic Magnetic Functional Complex and Nano Complex, School of Chemistry and Chemical Engineering, Anqing Normal University, Anqing 261433, China

[2] Pingyuan Laboratory, College of Chemistry, Zhengzhou University, Zhengzhou 450000, China

Nano Res., **Just Accepted Manuscript** • https://doi.org/10.26599/NR.2026.94908736

https://www.sciopen.com/journal/1998-0124 on Apr. 14, 2026

Just Accepted

TABLE OF CONTENTS (TOC)

Insert Table of Contents artwork here

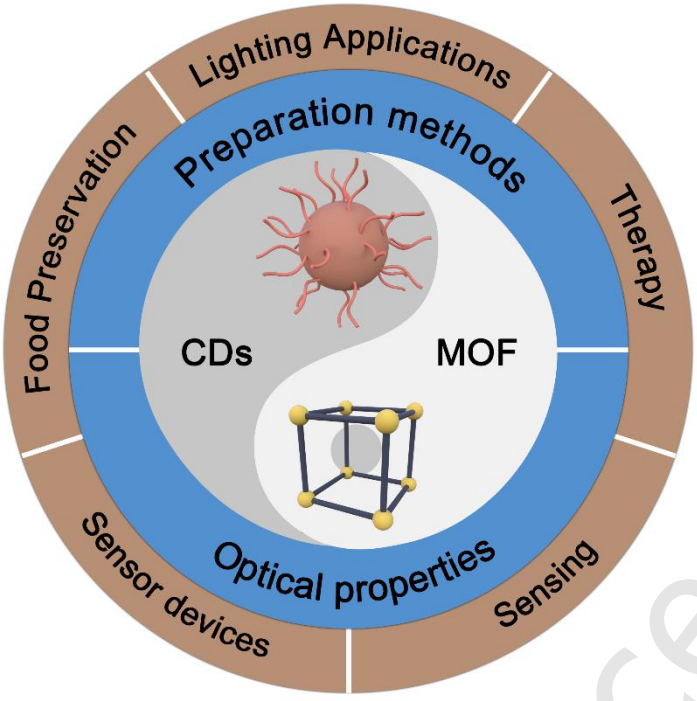

This review outlines recent advances in CDs@MOF composites, with emphasis on their construction strategies, interfacial structures, and luminescence regulation mechanisms under confinement effects.

Nano Research

Open Access

Review Article

Carbon dots@MOF composites: Synthetic strategies, luminescence regulation, and emerging applications

Boyang Wang[1], Nina Qian[1], and Siyu Lu [2]

[1] *Anhui Provincial Key Laboratory of Advanced Catalysis and Energy Materials, Anhui Key Laboratory of Optoelectronic Magnetic Functional Complex and Nano Complex, School of Chemistry and Chemical Engineering, Anqing Normal University, Anqing 261433, China*
[2] *Pingyuan Laboratory, College of Chemistry, Zhengzhou University, Zhengzhou 450000, China*

Received: 23 February 2026; **Revised:** 7 April 2026; **Accepted:** 14 April 2026

Address correspondence to Nina Qian, 162507@aqnu.edu.cn; Siyu Lu, sylu2013@zzu.edu.cn

Cite this article: *Nano Research*, 2026, 19, 94908736 https://doi.org/10.26599/NR.2026.94908736

ABSTRACT: Carbon dots (CDs) have attracted considerable attention due to their tunable luminescence, good biocompatibility, and environmental friendliness; however, they still suffer from limitations in solid-state stability and functional integration. Metal-organic frameworks (MOFs), characterized by highly ordered porous structures and designable metal nodes and organic ligands, provide an ideal platform for the construction of multifunctional composite materials. Integrating CDs with MOFs to form CDs@MOFs composites not only effectively suppresses aggregation-induced quenching of CDs through the rigid confinement effect of MOFs, but also enables precise regulation of the optical, chemical, and biological behaviors of CDs via interfacial coupling and structural engineering. This review systematically summarizes the main construction strategies of CDs@MOFs composites, with particular emphasis on the structural features and applicable scenarios of covalent and noncovalent coupling modes. On this basis, the mechanisms by which MOFs modulate the luminescent behavior of CDs, as well as the latest advances in their applications in sensing, lighting and display, food preservation, and biomedical therapy, are further discussed, highlighting the unique advantages of CDs@MOFs systems in multifunctional integration, structural tunability, and device-oriented applications. Finally, the current challenges faced by CDs@MOFs materials and their potential application prospects are proposed. We hope that this review will inspire new design concepts and provide valuable guidance for the future development of this promising field..

KEYWORDS: carbon dots, metal–organic frameworks, controlled synthesis, optical properties, applications

1 Introduction

In recent years, the rapid development of optoelectronic and luminescent functional materials has greatly promoted technological advances in displays, lighting, sensing, information security, and biomedicine [1-4]. As these applications increasingly demand high performance, environmental sustainability, and cost effectiveness, extensive efforts have been devoted to exploring novel material systems to improve device efficiency, stability, and functional integration [5-7]. Although conventional inorganic semiconductor quantum dots (e.g., CdTe and PbS), perovskite materials, and organic small-molecule emitters exhibit excellent optoelectronic properties, they often suffer from harsh synthesis conditions, high material costs, and concerns regarding environmental and biological safety, which significantly hinder their large-scale practical deployment [8-10]. Consequently, the development of alternative materials that combine superior optical performance with green sustainability and structural tunability has become a central research focus in the field of functional luminescent materials.

Carbon dots (CDs), as an emerging class of zero-dimensional carbon-based nanomaterials, have demonstrated remarkable potential in optoelectronic and luminescent applications owing to their broad spectral absornanoption, tunable emission behavior, high photostability, good biocompatibility, and solution processability [11-13]. Nevertheless, standalone CDs systems still face substantial challenges in achieving efficient solid-state emission, maintaining high emission efficiency, activating room-temperature phosphorescence, and realizing multifunctional integration [14-16]. In parallel, metal-organic frameworks (MOFs), featuring highly ordered porous architectures, tunable chemical compositions, and abundant metal – ligand functional sites, provide an ideal platform for constructing advanced hybrid luminescent systems [17-19]. Compared with other representative hybrid systems, such as perovskite@MOF and semiconductor quantum dot@MOF composites, CDs@MOF materials exhibit a distinct balance between performance, stability, and environmental compatibility [20]. Perovskite-based hybrids typically possess high photoluminescence quantum yields and narrow emission bandwidths, making them advantageous for high-performance optoelectronic applications; however, their intrinsic instability and toxicity (e.g., Pb-containing components) significantly limit practical deployment.

Semiconductor quantum dot@MOF systems also provide size-dependent emission and relatively high efficiency, but often involve heavy metals and limited surface tunability [21]. In contrast, CDs@MOF composites offer superior photostability, low toxicity, and rich surface functional groups, enabling flexible modulation of optical and chemical properties. These features make them particularly suitable for sensing, bio-related applications, and multifunctional platforms, although their relatively lower emission efficiency and broader spectra may restrict their use in applications requiring high color purity or lasing performance [22]. The integration of CDs with MOFs to form CDs@MOFs composites offers a new material design paradigm to overcome the intrinsic limitations of conventional CDs and to expand their functional scope [23].

Within CDs@MOFs systems, MOFs serve not merely as physical supports or host matrices, but actively modulate the structural evolution and photophysical processes of CDs through spatial confinement effects, interfacial interactions, and energy-level regulation. The rigid frameworks and nanoscale pores of MOFs effectively suppress aggregation-induced quenching and nonradiative decay of CDs under solid-state conditions, thereby enabling enhanced emission and efficient solid-state luminescence [24]. Moreover, the local microenvironments created by metal nodes and organic ligands can introduce spin-orbit coupling or rigidity-induced effects, facilitating triplet-state stabilization and radiative transitions, which ultimately activate long-lived room-temperature phosphorescence [25]. In addition, the high structural designability of MOFs endows CDs@MOFs composites with stimulus responsiveness, multimodal emission, and even chiroptical properties, conferring unique advantages in anticounterfeiting, lighting and display technologies, sensing, and biomedical applications [26].

Currently, significant progress has been achieved in the synthesis strategies, coupling modes, and optical regulation mechanisms of CDs@MOFs composites. However, most existing studies focus on specific material systems or single application scenarios, and a systematic understanding of the coupling configurations between CDs and MOFs, the structure-property relationships, and their general design principles across different application fields remains insufficient. Furthermore, although numerous reviews have separately summarized advances in CDs or MOFs for sensing and biomedical applications, comprehensive reviews dedicated to CDs@MOFs hybrid systems-covering material construction, luminescence regulation mechanisms, and multifunctional applications-are still relatively scarce.

Therefore, this review provides a systematic overview of the construction strategies and functional characteristics of CDs@MOFs composites. Particular emphasis is placed on the coupling modes between CDs and MOFs, the mechanisms by which MOFs regulate the luminescent behavior of CDs, and representative application advances in food preservation, lighting and display, sensing, and biomedicine. Finally, the current challenges related to emission efficiency, structural controllability, and device integration are critically analyzed, and future research directions are proposed, aiming to provide guidance for the rational design and practical application of CDs@framework hybrid materials.

Table 1. Comparison of preparation for CDs@MOFs.

Synthesis Method	Advantages	Limitations	Difficulty Level	Usage Frequency
Direct Reaction between CDs and MOFs	• Simple and efficient, suitable for large-scale synthesis • Direct interaction with MOF surfaces, providing relatively high stability • High flexibility, applicable to various CD–MOF combinations	• Poor dispersion of CDs, possible aggregation • Harsh reaction conditions may affect MOF structure and CDs properties	Moderate	High
Reaction between CDs and MOF Precursors	• Synergistic assembly, better preservation of MOF structural features • High-performance composites with tunable properties • High adaptability, allowing adjustment of precursor ratios	• More complex synthesis process, requiring precise control of reaction conditions • Large differences in precursor compatibility may influence the optical properties of CDs	Relatively difficult	High
Reaction between CDs Precursors and MOFs	• Straightforward synthesis process, time-saving • Efficient integration of CDs with MOFs, reduced cost • Enhanced interfacial compatibility between CDs and MOFs	• Non-uniform distribution of CDs, potentially affecting performance • Optical properties of CDs may be suboptimal; limited control over formation	Easy	Moderate
Reaction between CDs Precursors and MOF Precursors	• One-pot integrated synthesis, saving time and cost • Precise control over CD size and distribution • Improved optical performance and stability of the composites	• Complex process requiring precise control over multiple reaction parameters • Possible interference with MOF framework formation	Difficult	Low

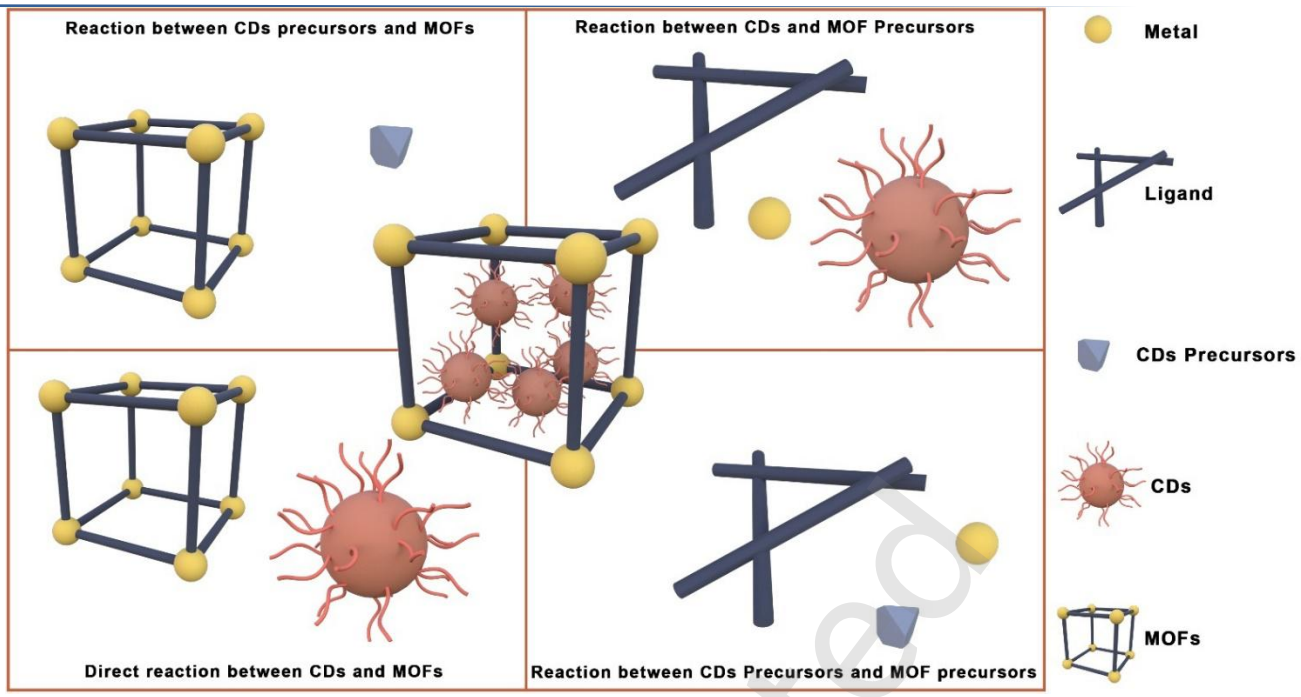

Figure 1. The strategies for the fabrication of CDs@MOFs.

2 Advantages of integrating CDs with MOFs

The integration of CDs with MOFs offers a unique structural and functional platform for the construction of next-generation multifunctional nanocomposites. Compared with single-component systems, the most prominent feature of composite materials lies in the synergistic integration of distinct functional units, which enables properties that are difficult to achieve by either component alone. CDs are a class of zero-dimensional carbon-based nanomaterials with a size of less than 10 nm [27]. Generally, CDs are considered to be composed of a core-shell structure. The core contains cross-linked structures and conjugated domains in different proportions, while the shell contains polymer structures and functional groups [28]. CDs feature controllable sizes, tunable luminescence, good biocompatibility, and facile surface functionalization; however, they are prone to aggregation-induced quenching and limited structural stability in solid-state applications. In contrast, MOFs possess highly ordered porous architectures, designable metal nodes and organic ligands, and excellent structural robustness, yet they typically lack efficient and tunable luminescent centers [29]. While both polymers and MOFs can provide a confined environment, MOFs offer several distinct features. First, MOFs possess highly ordered and tunable porous structures, which enable more precise control over spatial confinement compared to the relatively disordered polymer networks [30]. Second, the well-defined metal nodes and coordination environments in MOFs allow for additional regulation of photophysical processes, such as enhanced spin–orbit coupling or specific host-guest interactions, which are difficult to achieve in conventional polymer matrices [31]. Third, the crystallinity and structural uniformity of MOFs facilitate more reproducible structure-property relationships, which is beneficial for mechanistic understanding and rational design [32]. The combination of these two components not only leverages the rigid confinement and framework protection effects of MOFs to effectively suppress CDs aggregation and deactivation, but also enables precise regulation of the optical, electrical, and chemical behaviors of CDs through coordination interactions, energy transfer, and interfacial coupling. Moreover, the high specific surface area and well-defined pore channels of MOFs provide an ideal platform for reactant enrichment, mass-transport modulation, and multifunctional integration, while CDs act as efficient signal transducers or photoresponsive units that impart strong functional outputs. This complementary and synergistic integration endows CDs@MOFs systems with pronounced advantages in luminescence regulation, sensing, anticounterfeiting, lighting and display technologies, and biomedical applications. In addition, the composite architecture allows for multifunctional integration within a single platform. For example, CDs can provide optical signal output, while MOFs can simultaneously act as a structural scaffold, selective adsorbent, or catalytic center. Such functional complementarity is difficult to realize in individual materials

3 Preparation methods of CDs@MOFs

In studies on CDs@MOFs composites, the choice of synthetic strategy plays a critical role in determining the final structure, properties, and application performance of the resulting materials. To achieve effective integration of CDs with MOFs, a variety of preparation approaches have been developed, including direct reactions, precursor-mediated routes, and physical mixing strategies(**Figure 1**). Each method exhibits distinct characteristics and advantages during the synthesis process, enabling tailored control over the dispersion, stability, and optoelectronic properties of CDs according to specific application requirements (**Table 1**).

3.1 Direct reaction between CDs and MOFs

The direct reaction between CDs and MOFs represents a simple and efficient synthesis strategy that is well suited for

large-scale preparation [33]. Typically, pre-synthesized CDs are directly mixed with pre-formed MOFs under appropriate reaction conditions. With the assistance of heating, solvent effects, or catalysts, the CDs can be uniformly dispersed and stably embedded within the pores of the MOFs or anchored onto their surfaces [34]. In general, direct CDs – MOFs integration to construct CDs@MOFs composites can be classified into two main approaches. The first relies on physical mixing driven by electrostatic interactions between oppositely charged CDs and MOFs [35]. As illustrated in **Figure 2a**, a MIL-101-type MOF was synthesized via a self-assembly strategy using chromium nitrate and terephthalic acid as precursors [36]. The as-prepared MIL-101 was then dispersed in ethanol, followed by the addition of CDs and continuous mechanical stirring to obtain CDs@MIL-101 composites. UiO-66, a positively charged MOF (+21.9 mV), can be efficiently combined with negatively charged CDs through electrostatic attraction to form CDs@UiO-66. Furthermore, by employing UiO-66-NH_2 with a higher positive surface charge (+41.3 mV) and folic-acid-modified CDs bearing enhanced negative charge, the coupling efficiency of the composite can be further improved [37]. In another example, Zhang et al. physically mixed CDs with NAR@ZIF-8 and subsequently fabricated composite fibers via electrospinning [38]. By varying the contents of CDs and NAR@ZIF-8, the electrical conductivity, viscosity, and surface tension of the spinning solution could be tuned, thereby regulating the morphology and diameter of the resulting fibers (**Figure 2b**). The second approach involves post-synthetic modification using EDC/NHS chemistry to covalently link CDs and MOFs [39]. In this strategy, EDC activates carboxyl groups on the surface of CDs or MOFs to form unstable o-acylisourea intermediates, which are prone to hydrolysis. The introduction of NHS converts these intermediates into more stable NHS esters with high affinity toward amino groups, significantly enhancing the efficiency of subsequent amide bond formation with –NH_2 functionalities. As a result, the EDC/NHS system has been widely employed as a representative "zero-length" crosslinking strategy for covalent coupling between CDs and MOFs. For instance, Chun et al. formed covalent bonds between the amino groups of UiO-66-NH_2 and the carboxyl groups of CDs, thereby functionalizing UiO-66-NH_2 with CDs to construct heterojunction composites (**Figure 2c**) [40].

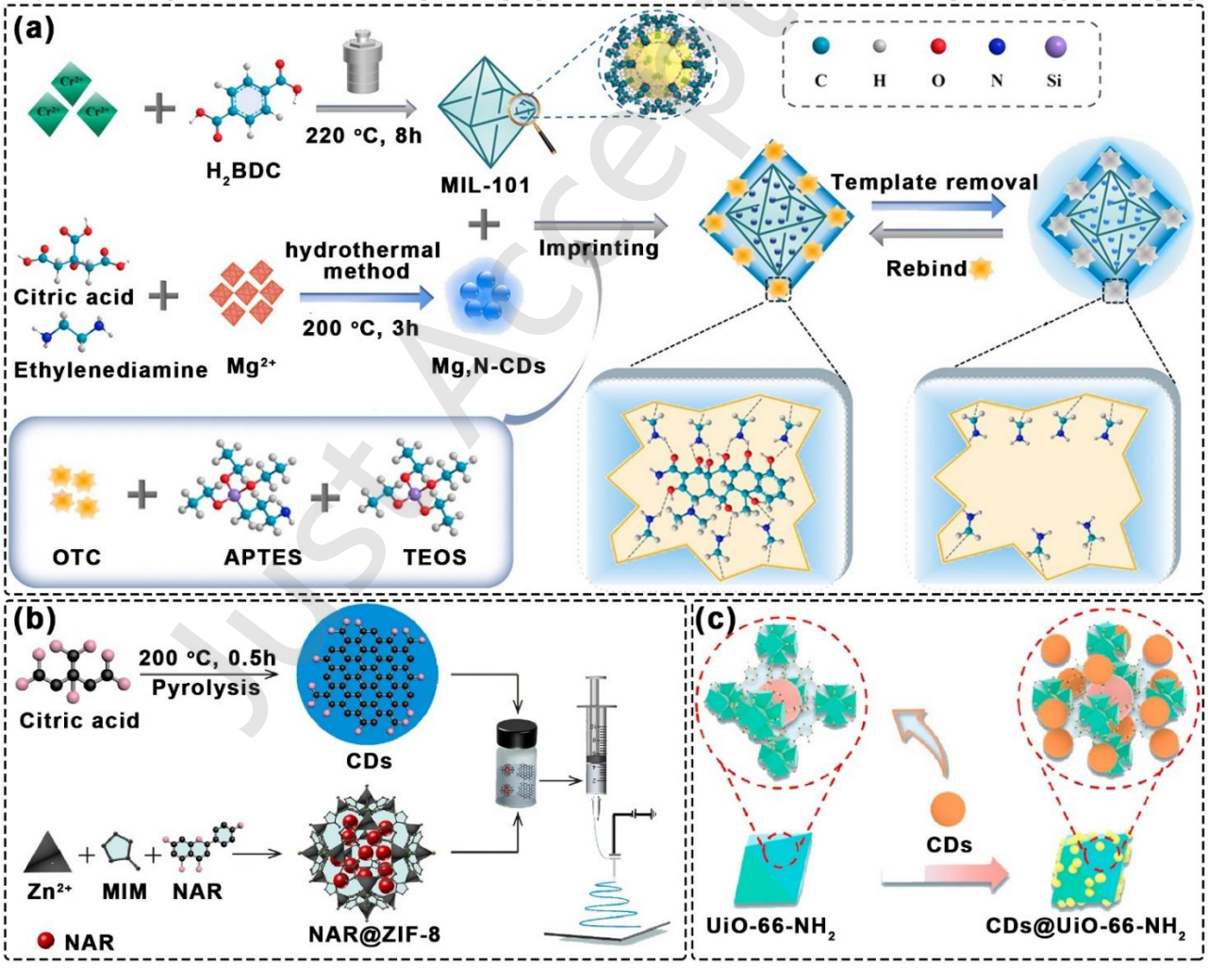

Figure 2. Prepared CDs@ MOFs by reaction between CDs and MOFs. (a) Physical mixing. Reproduced with permission from Ref. [36], Copyright Elsevier, 2023. (b) Electrostatic adsorption. Reproduced with permission from Ref. [38], Copyright Elsevier, 2023. (c) Post-modification. Reproduced with permission from Ref. [40], Copyright Elsevier, 2023.

3.2 Reaction between CDs and MOF Precursors

The reaction between CDs and MOF precursors (such as metal salts and organic ligands) is typically carried out by introducing CDs as functional components during the MOF

synthesis process, allowing them to interact with metal ions or organic linkers before the complete formation of the MOFs crystalline framework [41, 42]. Compared with direct mixing strategies, this approach enables CDs to participate in the nucleation or early growth stages of MOFs, thereby promoting more homogeneous incorporation within the framework [43, 44]. Moreover, the abundant surface functional groups of CDs (e.g., amino, carboxyl, and hydroxyl groups) can effectively coordinate with metal precursors, enhancing the structural stability of the composites, reducing the likelihood of post-synthetic leaching, and largely preserving the intrinsic structural characteristics of the MOFs [45, 46]. Wang et al. introduced CDs during the synthesis of MOFs, where the CDs acted as internal nucleation templates and the MOFs self-assembled around them. Scanning electron microscopy (SEM) analysis showed that the pristine MOFs exhibited a well-defined rhombic octahedral morphology [47]. After the incorporation of CDs, the morphology of the resulting CDs@MOFs composites changed significantly. With increasing CDs content, the MOFs surface evolved from smooth to rough, accompanied by a gradual decrease in particle size. This trend highlights the crucial role of CDs as nucleation regulators, which interfere with crystal growth and thereby modulate the size and surface texture of the resulting MOFs structures (**Figure 3a**). Ha et al. prepared CD@MOF composites using zirconium clusters as the metal nodes and biphenyl-4,4′-dicarboxylic acid (H_2bpdc) as the organic linker. The structures of the CDs@MOFs composites were investigated by SEM and transmission electron microscopy (TEM). The pristine MOFs exhibited a nanoflower-like morphology, and the CDs@MOFs composites displayed a similar nanoflower-like structure with a slightly larger size than that of the original MOFs [48]. These observations indicate that the introduction of CDs did not disrupt the intrinsic MOFs framework. TEM analysis further confirmed the presence of CDs within the CDs@MOFs composites (**Figure 3b**). Using an ultrasound-assisted method, Boonmak et al. incorporated CDs into benzene-1,3,5-tricarboxylic acid to fabricate CDs@HKUST-1 composites [49]. Owing to the large pore size and functionalized pore surfaces of HKUST-1, the framework can not only serve as a host for loading CDs but also capture guest molecules. Notably, the emission intensity of the as-prepared CDs@HKUST-1 was very weak, which was attributed to energy transfer from the CDs to the Cu^{2+} centers in HKUST-1 (**Figure 3c**). In another study, CDs were embedded into the three-dimensional porous structure during the growth of ZIF-8, enabling the in-situ preparation of highly luminescent CDs@ZIF-8 nanocomposites [50]. The formation of CDs@ZIF-8 is believed to arise from coordination interactions between Zn^{2+} and N-containing groups or terminal carboxyl groups on the surface of CDs during the growth of the ZIF-8 framework (**Figure 3d**).

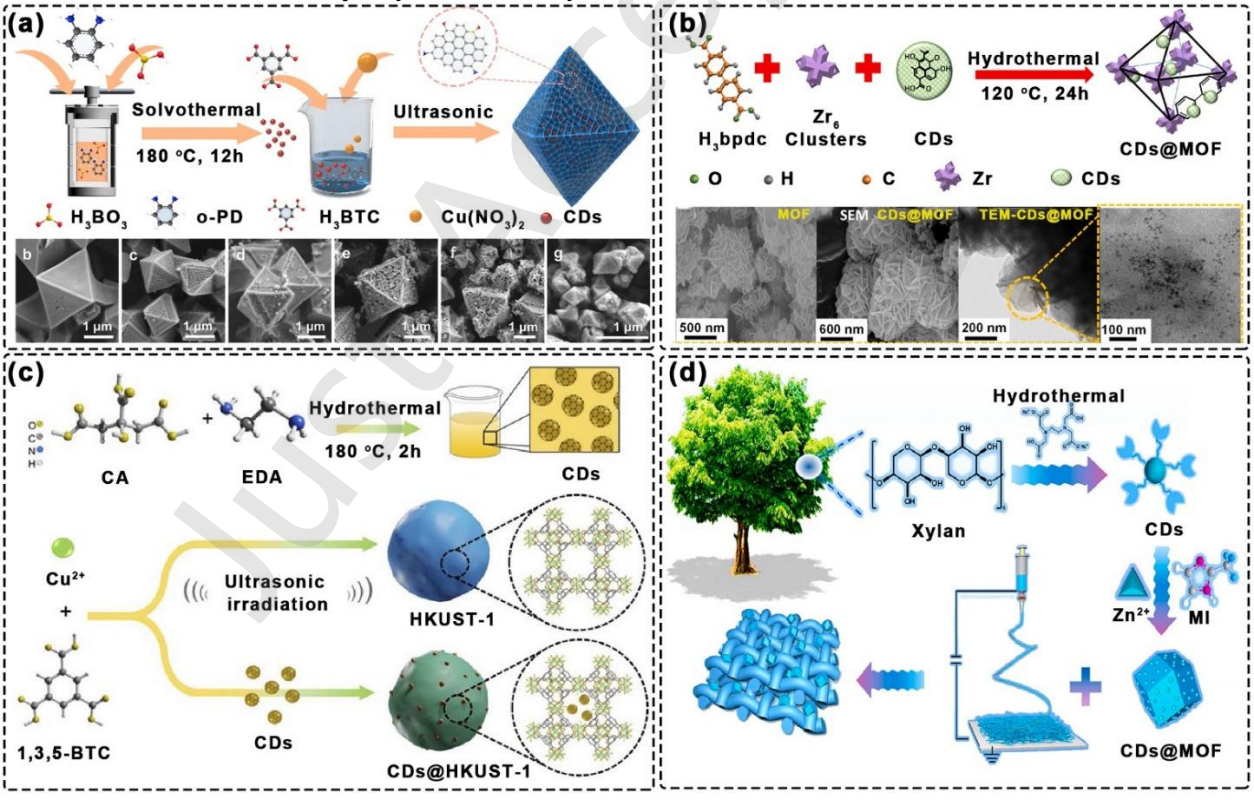

Figure 3. Prepared CDs@ MOFs by reaction between CDs and MOF precursors. (a) CDs act as nucleation regulators during MOFs crystallization. Reproduced with permission from Ref. [47], Copyright Elsevier, 2026. (b) CDs incorporation preserves the intrinsic MOFs nanoflower architecture. Reproduced with permission from Ref. [48], Copyright Elsevier, 2024. (c) Interfacial energy transfer quenches CDs emission in HKUST-1. Reproduced with permission from Ref. [49], Copyright Royal Society of Chemistry, 2022. (d) Coordination interactions enable in situ confinement of CDs in ZIF-8. Reproduced with permission from Ref. [50], Copyright Elsevier, 2023.

3.3 Reaction between CDs precursors and MOFs

This strategy involves introducing CDs precursors into preformed MOFs, allowing the confined microenvironment of the MOF to participate in and regulate the carbonization

process [51]. Small-molecule or polymeric precursors are first infiltrated into the pores or channels of the MOF, followed by thermal, hydrothermal, or chemical treatments to induce in situ carbonization, yielding CDs with spatial confinement and structures templated by the host framework. Benefiting from the well-defined porosity and chemical tunability of MOFs, this approach enables precise control over the nucleation sites, size distribution, and surface functionalities of the resulting CDs [52]. Moreover, because carbonization occurs within or on the surface of the MOF architecture, the obtained CDs@MOFs composites typically exhibit intimate interfacial contact and enhanced electronic or catalytic coupling. This method is particularly attractive when precise control over the size or spatial distribution of CDs is required. MIL-53(Fe) features diamond-like channels that facilitate the ingress and enrichment of small molecules. Li et al. impregnated glucose molecules into MIL-53(Fe) via an impregnation method [53]. Because the internal pore surface area of the MOF particles is much larger than the external surface area, most glucose molecules are physically adsorbed inside the MOF channels, while only a small fraction is adsorbed on the external surface and can be readily removed by washing. Upon heating the glucose-loaded MIL-53(Fe), glucose undergoes carbonization under the confinement of the MOF channels to form CDs (**Figure 4a**).

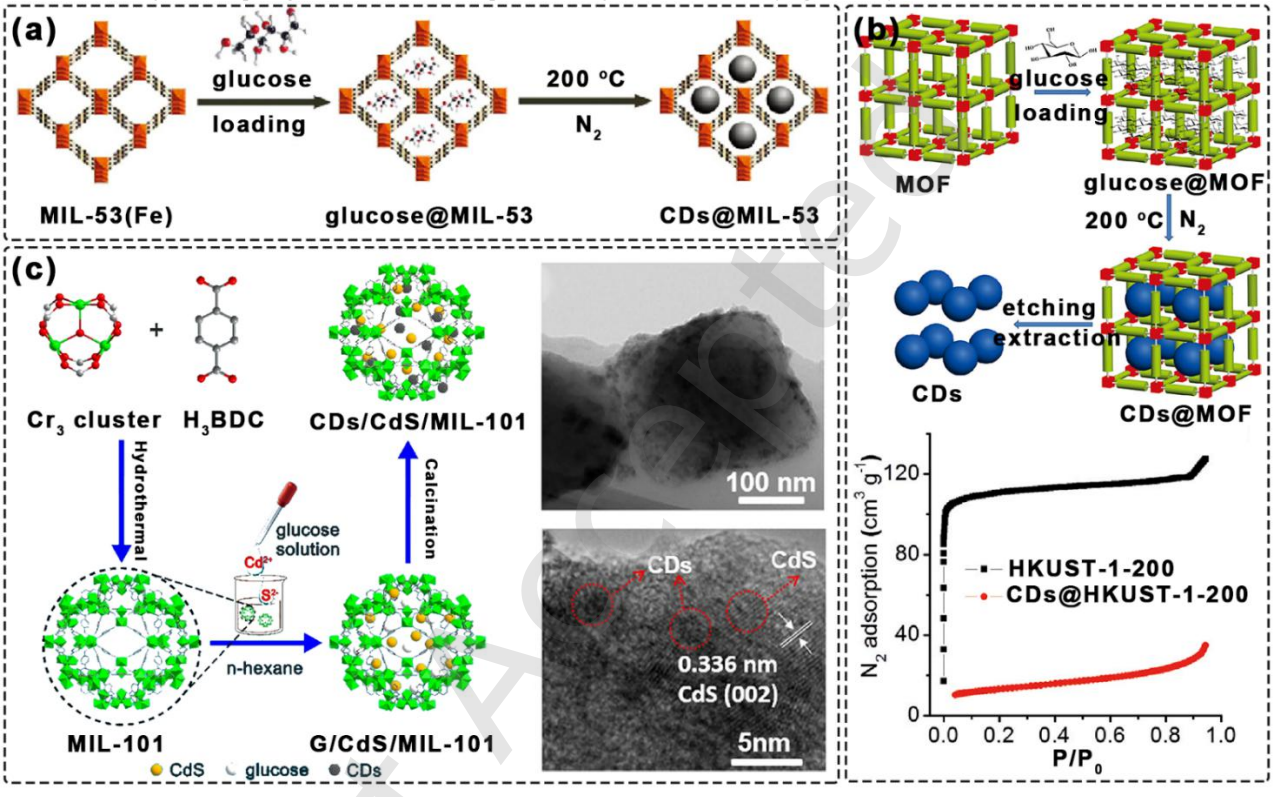

Figure 4. Prepared CDs@ MOFs by reaction between CDs precursors and MOF. (a) In situ carbonization of glucose confined within MIL-53(Fe) channels. Reproduced with permission from Ref. [53], Copyright Royal Society of Chemistry, 2018. (b) Pore-confined formation of ordered CDs arrays inside HKUST-1 frameworks. Reproduced with permission from Ref. [54], Copyright Wiley, 2017. (c) MOFs-confined nanoreactor synthesis of CDs/CdS@MIL-101 composites. Reproduced with permission from Ref. [55], Copyright Elsevier, 2019.

Furthermore, Zhang et al. loaded glucose molecules into the pores of MOFs and subsequently calcined the composites [54]. Owing to the thermal stability of the MOFs at the applied temperature, the resulting CDs were confined within the MOFs pores, yielding structurally ordered CDs arrays, denoted as CDs@MOFs. After calcination, the N_2 adsorption capacity of CDs@HKUST-1-200 decreased dramatically from approximately 130 cm^3 g^{-1} for pristine HKUST-1 to about 5 cm^3 g^{-1}, indicating that most of the internal pores of HKUST-1 were occupied by CDs (**Figure 4b**). By co-incorporating CdS quantum dots and CDs into MOFs pores, ternary composites can be constructed using the MOF cavities as nanoreactors. In this approach, Cd^{2+}, S^{2-}, and carbon-dot precursors were simultaneously introduced into the pores of MIL-101 via a one-step dual-solvent method, followed by thermal treatment. As shown in **Figure 4c**, TEM images of CDs/CdS@MIL-101 clearly reveal that ultrasmall nanoparticles are embedded within the MIL-101 nanocrystals without severe aggregation [55].

3.4 Reaction between CDs Precursors and MOF precursors

In this bottom-up co-assembly strategy, CDs precursors and MOFs precursors react simultaneously, enabling the synchronous formation of CDs and the MOFs. This one-pot synthetic route allows the carbonization process and MOFs crystallization to mutually influence each other, thereby establishing robust and homogeneous integration at an early stage of material construction [56, 57]. During the reaction, CDs can nucleate within the evolving coordination network or at the interfaces between metal ions and organic linkers, leading to composite materials with highly interconnected architectures. The morphology, composition, and defect structure of the resulting CDs@MOFs can be finely tuned by adjusting precursor ratios, reaction temperature, or solvent

conditions [58]. Omer et al. reported an approach for the in-situ encapsulation of CDs within the pores of MOFs [59]. In this process, luminescent CDs are generated in situ and subsequently trapped inside the MOF cavities, yielding CDs@MOFs composites. The CDs@MOFs exhibit bright blue emission, with emission bands attributable to both the MOF ligand and the confined CDs, indicating successful encapsulation of CDs within the MOFs pores (**Figure 5a**). Xu et al. demonstrated a synthetic route to CDs@UiO-66(OH)$_2$. Using $ZrOCl_2 \cdot 8H_2O$ as the metal precursor, 2,5-dihydroxyterephthalic acid as the organic linker, and tetraethylammonium bromide as a template, CDs were generated in situ during a co-thermal process and simultaneously encapsulated within the UiO-66(OH) $_2$ (**Figure 5b**) [60].

The direct reaction between CDs and MOFs method is considered the most suitable for large-scale production due to its operational simplicity, mild conditions, and compatibility with existing MOF synthesis protocols [61]. In contrast, strategies involving precursor-mediated in situ growth generally offer better interfacial integration and structural control, but may face challenges in scale-up due to more complex reaction conditions, sensitivity to synthesis parameters, and potential batch-to-batch variability [62].

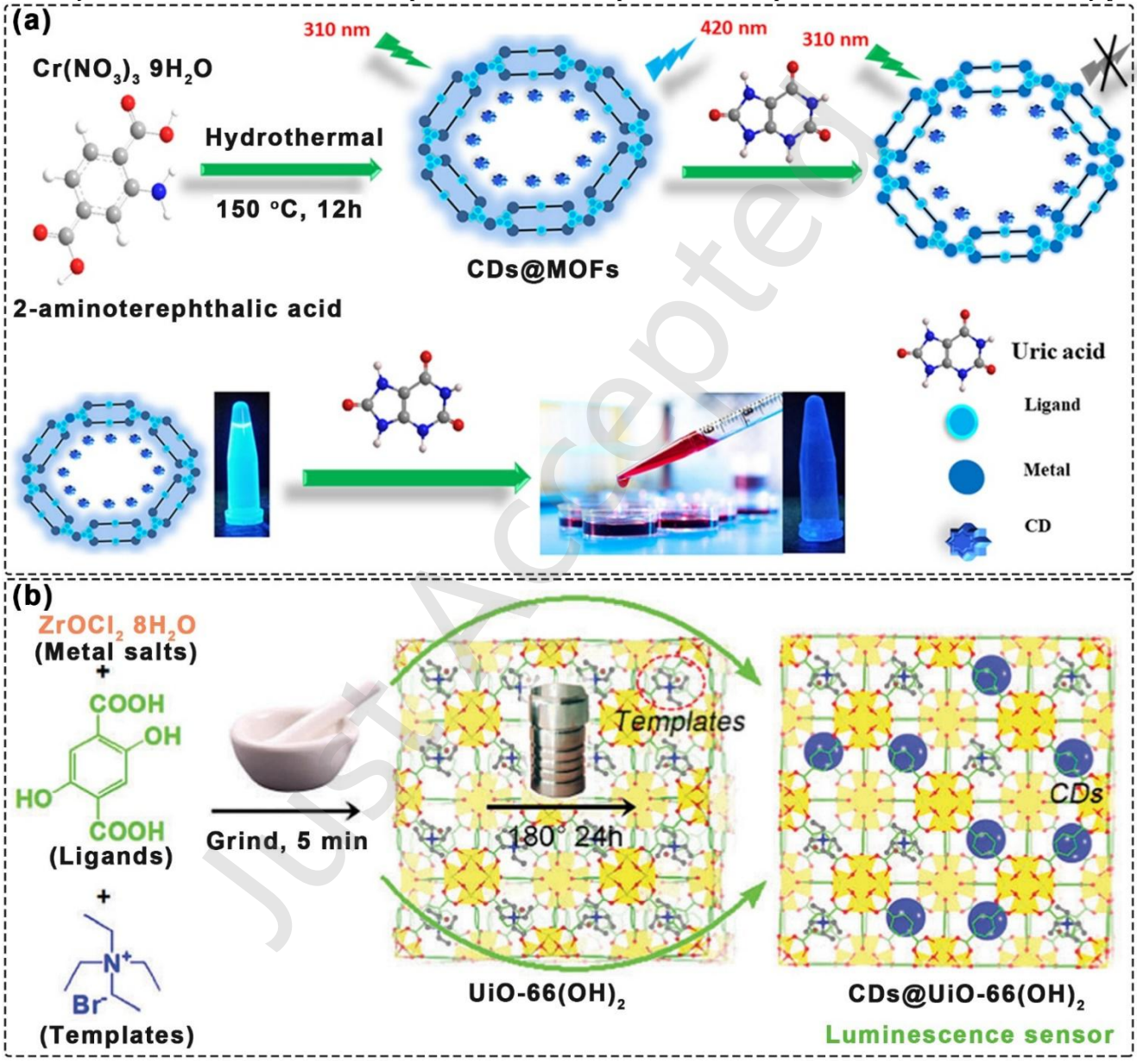

Figure 5. Prepared CDs@ MOFs by reaction between CDs precursors and MOF precursors. (a) One-pot co-assembly generating in situ CDs encapsulated within MOF pores. Reproduced with permission from Ref. [59], Copyright American Chemical Society, 2022. (b) One-pot co-assembly yielding in situ CDs confined in UiO-66(OH)2. Reproduced with permission from Ref. [60], Copyright Royal Society of Chemistry, 2018.

4 Influence of MOFs on the luminescent behavior of CDs

MOFs provide a confined and rigid microenvironment that regulates the excited-state dynamics of CDs. By restricting molecular motion, suppressing nonradiative decay, and

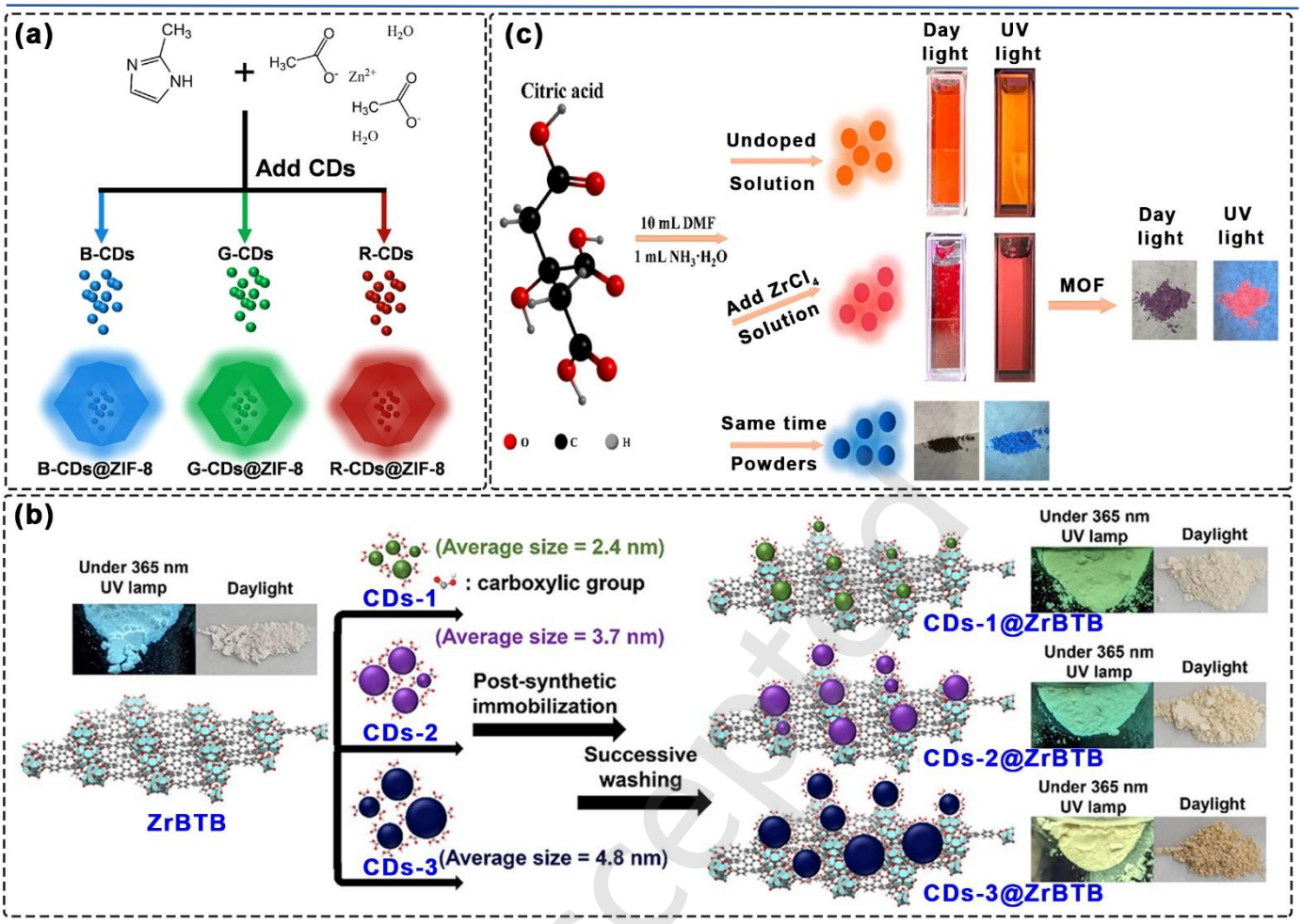

Figure 6. MOF-regulated solid-state luminescence of CDs. (a) Pore confinement suppresses aggregation-caused quenching of CDs. Reproduced with permission from Ref. [67], Copyright Wiley, 2024. (b) Framework immobilization reduces charge migration and nonradiative decay. Reproduced with permission from Ref. [69], Copyright Springer, 2024. (c) Rigid coordination environment stabilizes emissive states and enhances quantum yield. Reproduced with permission from Ref. [71], Copyright Elsevier, 2024.

stabilizing excited states, MOFs enable CDs to access emission pathways that are difficult to achieve in isolated systems, including solid-state luminescence, room-temperature phosphorescence (RTP), and chiral emission. These effects primarily arise from spatial confinement, interfacial passivation, and energy-level modulation.

4.1 MOF-promoted solid-state luminescence of CDs

Solid-state emission of CDs is typically limited by aggregation-caused quenching. MOFs alleviate this issue by spatially isolating CDs within porous frameworks and immobilizing them, thereby reducing nonradiative losses. This confinement enables efficient solid-state luminescence [63-65]. First, when CDs are embedded within MOF micropores, the interparticle distance between CDs is forcibly increased, thereby preventing direct stacking and reducing excitation energy dissipation [66]. For example, Li et al. employed ZIF-8 as an efficient encapsulation matrix to confine CDs, allowing the CDs to preserve their intrinsic fluorescence characteristics and yielding solid-state fluorescent CDs@ZIF-8 powders. Upon hybridization with ZIF-8, the MOF can absorb incident light and transfer the excitation energy to the CDs, thereby enhancing their excitation efficiency. In addition, ZIF-8 may improve the overall light-harvesting capability of the composite. Furthermore, charge transfer from ZIF-8 to CDs may occur, altering the band structure of CDs and facilitating radiative recombination under specific excitation wavelengths, which collectively contributes to enhanced solid-state luminescence (**Figure 6a**) [67]. Second, the rigid frameworks of MOFs can immobilize the position and orientation of CDs, thereby suppressing charge migration between adjacent emitters and reducing nonradiative decay pathways [68]. In post-synthetic immobilization strategies, CDs bearing terminal carboxyl groups can coordinate with terminal hydroxyl groups on ZrBTB, effectively anchoring the CDs within the framework. Kung et al. demonstrated the immobilization of CDs with three different sizes and successfully synthesized a series of solid-state emissive CDs@MOFs (**Figure 6b**) [69]. Third, the rigidity of MOFs structures can further weaken interactions among surface functional groups of CDs, enabling the composites to maintain high luminescence efficiency in the solid state [70]. Gong et al. prepared solid-state emissive CDs@MOFs composites using anhydrous citric acid as the carbon precursor and $ZrCl_4$ as both the metal source and an inorganic salt matrix. The amount of $ZrCl_4$ was found to strongly influence the interaction between the rigid

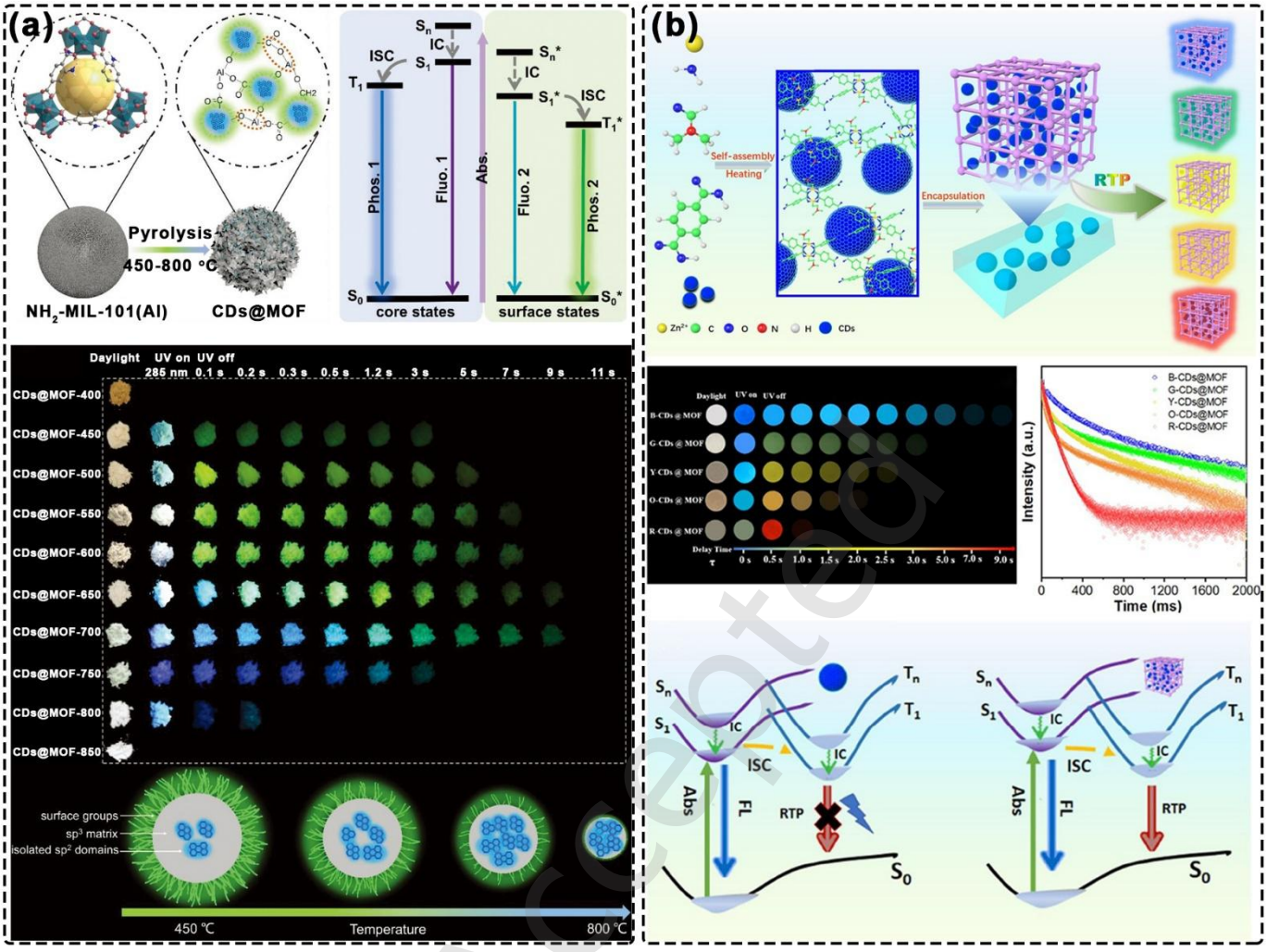

Figure 7. MOF-enabled RTP regulation in CDs@MOF composites. (a) Rigid confinement-induced ISC enhancement and triplet-state stabilization. Reproduced with permission from Ref. [75], Copyright Wiley, 2023. (b) Heavy-atom-assisted spin-orbit coupling for tunable RTP emission. Reproduced with permission from Ref. [77], Copyright American Chemical Society, 2022.

framework and CDs. The photoluminescence quantum yield of the resulting CDs@MOFs initially increased with increasing $ZrCl_4$ content and subsequently decreased, highlighting the critical role of framework rigidity and coordination environment in regulating solid-state emission (**Figure 6c**) [71].

4.2 MOF-promoted room-temperature phosphorescence of CDs

RTP in CDs is hindered by oxygen quenching and rapid nonradiative decay. The rigid and confined environment of MOFs suppresses molecular motion and limits oxygen diffusion, facilitating intersystem crossing and stabilizing triplet states, thus enabling RTP emission [72-74]. For example, Hu et al. employed an aluminum-based MOF as the precursor for constructing CDs@MOFs composites, in which the organic ligands served as carbon sources for cross-linked carbonization [75]. The porous architecture of the MOF imposed spatial confinement on the CDs, thereby enhancing RTP emission. The RTP behavior was found to be strongly dependent on the synthesis temperature. At relatively low temperatures, the organic linkers in the MOF could not be converted into CDs. With increasing temperature, surface-state emissive centers formed, although the carbon core was not yet fully carbonized. Upon further temperature elevation, a large number of isolated sp^2-conjugated domains were generated within the sp^3-dominated carbon matrix, accompanied by the partial decomposition of surface functional groups, resulting in the most pronounced RTP emission. Excessively high temperatures, however, led to oxidation of these isolated sp^2 domains, reducing the number of core emissive centers and consequently weakening the RTP intensity (**Figure 7a**). In addition, the metal ions and organic linkers of MOFs may introduce the "heavy-atom effect," which enhances spin-orbit coupling and thereby promotes more efficient ISC, facilitating the formation of long-lived triplet states in CDs [76]. Meng et al. embedded CDs into MOFs containing heavy metal ions, exploiting their ability to modulate triplet energy levels and further enhance ISC [77]. As a result, CDs@MOFs composites exhibiting tunable RTP emission wavelengths ranging from blue to red, as well as adjustable phosphorescence lifetimes, were successfully achieved. Notably, these CDs@MOFs displayed excellent photostability, with both photoluminescence and RTP

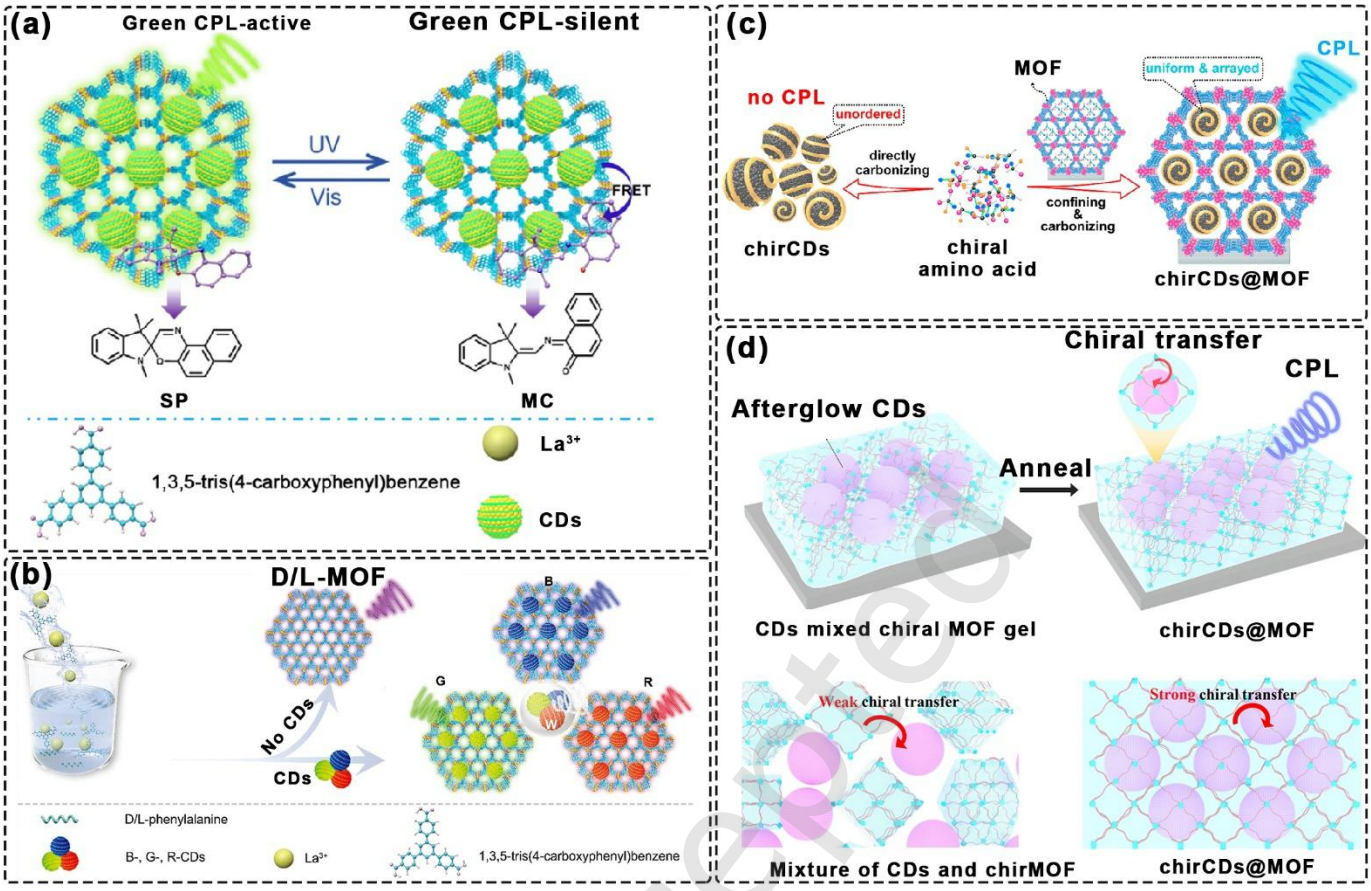

Figure 8. MOF-induced chirality of CDs. (a) Chiral MOF–induced CPL via confined CDs/SP photochromic assemblies. Reproduced with permission from Ref. [80], Copyright Royal Society of Chemistry, 2025. (b) Chirality inheritance in CDs confined within enantiomeric MOFs. Reproduced with permission from Ref. [81], Copyright Wiley, 2024. (c) Confinement-stabilized chiral CDs generated by MOF-templated carbonization. Reproduced with permission from Ref. [83], Copyright American Chemical Society, 2023. (d) Circularly polarized RTP enabled by chiral CDs@MOFs composite films. Reproduced with permission from Ref. [84], Copyright Springer, 2025.

intensities showing only slight attenuation even after 10 h of continuous excitation (**Figure 7b**).

4.3 MOF-induced chirality of CDs

Chiral MOFs or asymmetric confinement environments can induce chiroptical activity in CDs by perturbing their electronic structures and restricting conformational freedom. This enables circular dichroism and circularly polarized luminescence in otherwise achiral systems [78,79]. Zhang et al. co-encapsulated CDs and spiropyran (SP) into chiral MOF to construct CDs-based photochromic solid-state circularly polarized luminescence (CPL) assembly [80]. Under alternating ultraviolet and visible-light irradiation, the SP units within the CDs@MOF/SP assembly reversibly switched between a colorless closed-ring form and a blue open-ring form. This transformation selectively deactivated or activated the photochromic fluorescence resonance energy transfer between CDs and SP, enabling reversible optical switching of both photoluminescence and CPL signals (**Figure 8a**). By selecting a pair of violet-emissive enantiomeric lanthanide-based MOFs (D/L-MOF) as chiral hosts, full-color CDs were confined within the MOF to form D/L-CDs@MOF assemblies [81]. The uniformly encapsulated CDs not only overcame aggregation-caused quenching in the solid state but also inherited the chirality of the parent MOF, resulting in pronounced chiroptical activity (**Figure 8b**). Moreover, the confinement effect of MOFs can enforce specific spatial orientations of CDs and reduce their conformational freedom, thereby stabilizing chiral conformations [82]. In this context, asymmetric arrangements of the carbon core or surface functional groups of CDs may become fixed, leading to circular dichroism or CPL responses. Zhang et al. employed a liquid-phase epitaxial layer-by-layer strategy to fabricate achiral porous pyrene-based MOF films as host templates [83]. Chiral amino acids were confined within the MOFs pores as carbon precursors and subsequently carbonized to generate uniform arrays of ultrasmall chiral CDs, yielding chiral CDs@MOFs film. In contrast to CDs obtained by direct carbonization of chiral amino acids, which exhibited negligible CPL activity, effective excited-state chirality transfer was achieved in chirCDs@MOFs due to array confinement and coordination interactions between chirCDs and MOFs (**Figure 8c**). Gu et al. further realized circularly polarized RTP by synthesizing chirCDs@MOFs composite films via a gel-to-film conversion strategy. In the resulting chirCDs@MOFs films, the chiral MOF provided an asymmetric environment, while CDs served as the afterglow emitters embedded within the framework [84]. The strong chirality transfer and the seamless integration between chiral nanoparticles and chiral MOFs were identified as key

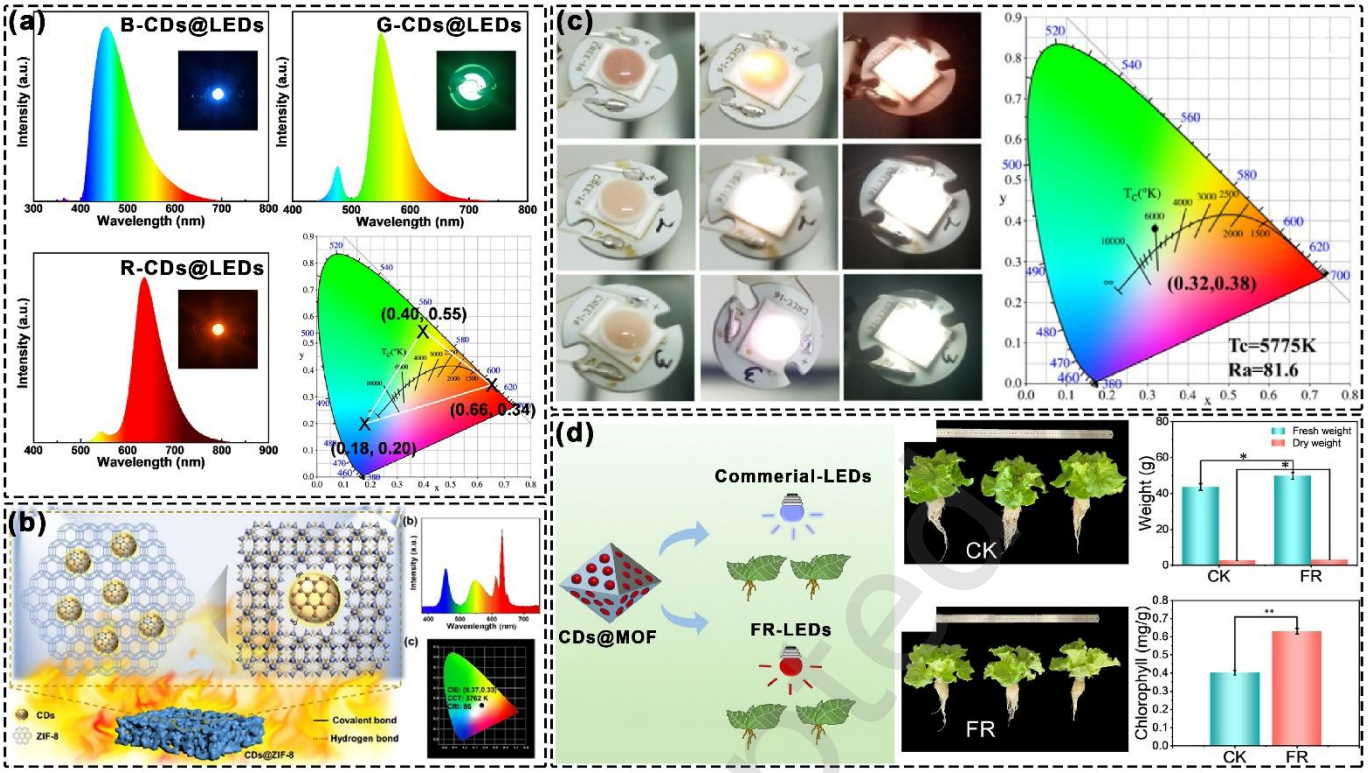

Figure 9. Lighting applications of CDs@MOFs. (a) Multi-color LEDs. Reproduced with permission from Ref. [67], Copyright Wiley, 2024. (b) White LEDs. Reproduced with permission from Ref. [93], Copyright Elsevier, 2024. (c) Cool white to warm white LEDs. Reproduced with permission from Ref. [94], Copyright Elsevier, 2019. (d) CDs@MOFs used for plant-growth lighting. Reproduced with permission from Ref. [95], Copyright Royal Society of Chemistry, 2023.

factors enabling high circularly polarized afterglow emission. By contrast, simple physical mixtures of powdered chiral MOFs and CDs exhibited large interfacial gaps and failed to display CPL behavior. (**Figure 8d**)

5 Optical Applications of CDs@MOFs

Benefiting from the outstanding optical properties of CDs and the high structural tunability of MOFs, CDs@MOFs composites have demonstrated remarkable advantages across multiple application fields [85]. The confinement effect, adjustable pore architecture, and metal ions of MOFs endow the composite systems with enhanced stability, selectivity, and interfacial activity, while the intrinsic fluorescence, versatile surface chemistry, and good dispersibility of CDs provide optical and chemical responsiveness [86]. Owing to this synergistic integration, CDs@MOFs have experienced rapid development in sensing, optoelectronic devices, and biomedical applications [87-89]. In sensing, CDs@MOFs exploit their high specific surface area and multiple recognition sites to enable sensitive detection of ions, small molecules, and gases. In optical and luminescent devices, these composites can achieve stable and bright solid-state emission, rendering them promising solution-processable emissive layers for next-generation light-emitting diodes (LEDs). In biomedical applications, CDs@MOFs integrate favorable biocompatibility, fluorescence imaging capability, and drug-loading potential, enabling multifunctional platforms for imaging, controlled release, and therapy.

5.1 Lighting Applications

CDs@MOF composites have emerged as promising materials for lighting and display applications owing to their tunable emission properties, excellent solid-state stability, and structural designability [90]. The rigid framework and confinement effect of MOFs effectively suppress aggregation-induced quenching of CDs in solid or film states, thereby preserving efficient luminescence, while CDs serve as the primary emissive centers, providing broadband tunable emission and high color purity [91]. In LEDs construction, CDs@MOFs function as emissive layers in which the emission wavelength, intensity, and energy-transfer processes of CDs can be precisely regulated through rational design of MOF pore structures, metal nodes, and organic linkers, enabling the realization of stable monochromatic or white LEDs [92]. By optimizing the amount of $ZrCl_4$ during CD synthesis, the emission wavelength of the resulting CDs can be red-shifted from 596 to 650 nm. Encapsulation of CDs within MOFs yields optically stable CD@MOF phosphors that can be used to fabricate red LEDs. When the driving current is increased from 20 to 100 mA, the emission peak position remains nearly unchanged, and only a slight decrease in intensity is observed, indicating excellent operational stability of the red LEDs [71]. Gong et al. fabricated three monochromatic LEDs using three different CDs@ZIF-8 phosphors. Distinct blue, green, and red emission peaks were clearly observed in the electroluminescence spectra [67]. The triangular region formed by the corresponding color coordinates encloses the white light region, demonstrating that multicolor and even white LEDs can be achieved by adjusting the mixing ratio of the three CDs@ZIF-8 phosphors (**Figure 9a**). Liu et al. prepared yellow-emissive

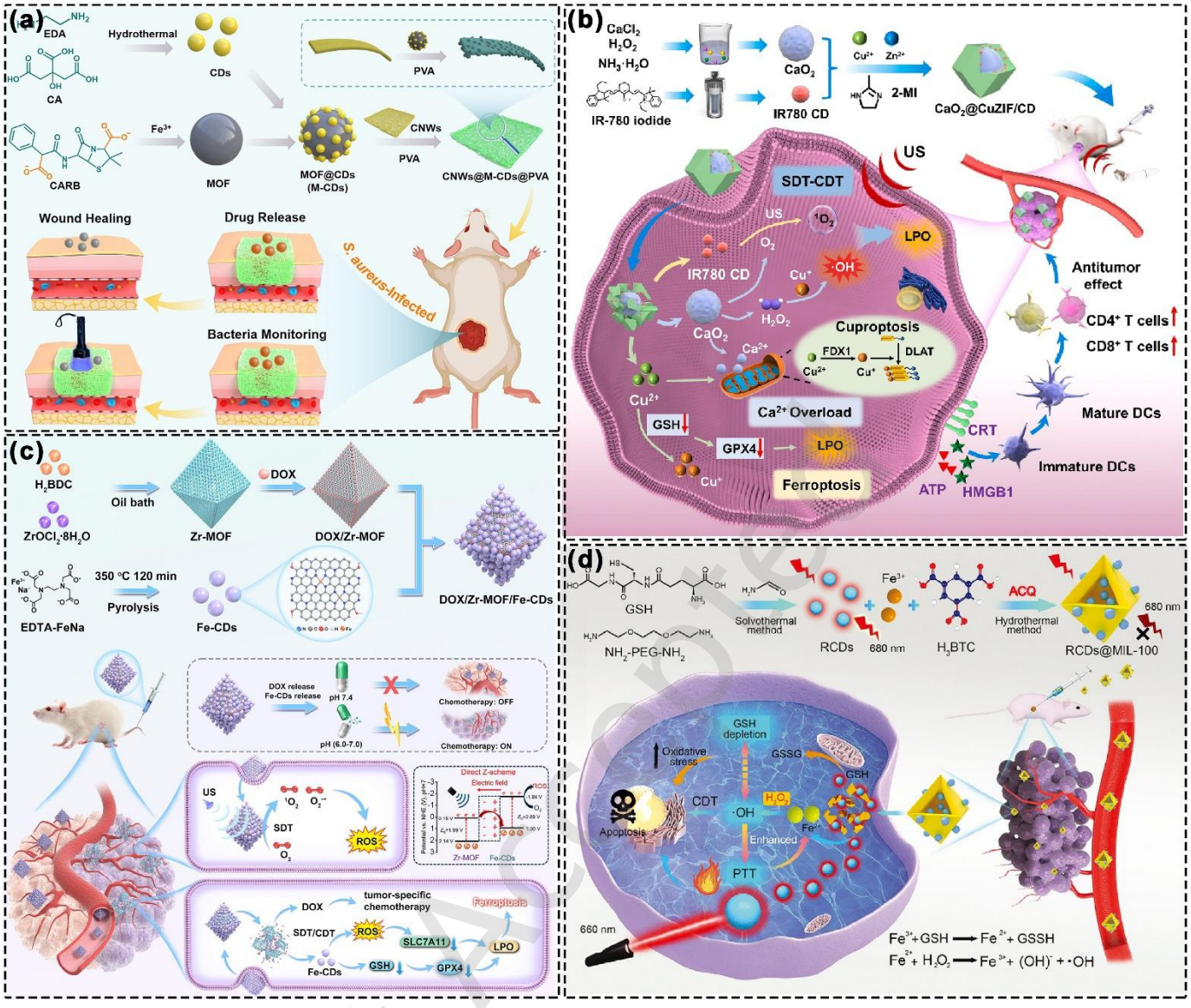

Figure 10. CDs@MOFs are used for therapy. (a) Wound healing. Reproduced with permission from Ref. [102], Copyright Wiley, 2025. (b) Cuproptosis-Ferroptosis. Reproduced with permission from Ref. [104], Copyright Elsevier, 2025. (c) Photothermal and photodynamic therapy. Reproduced with permission from Ref. [105], Copyright Wiley, 2025. (d) Multimodal synergistic therapy. Reproduced with permission from Ref. [106], Copyright Wiley, 2022.

CDs@MOFs via electrostatic adsorption. The resulting CDs@MOFs exhibited a high photoluminescence quantum yield of 81.17% and retained 100% and 80% of its fluorescence intensity after prolonged light irradiation (60 min) and high-temperature treatment (478 K), respectively [93]. Using CDs@ZIF-8 as a phosphor combined with a 450 nm blue laser diode, a white LEDs was constructed, exhibiting chromaticity coordinates of (0.37, 0.33) (**Figure 9b**). Ren et al. synthesized two types of CDs@MOFs via different routes: a two-step method involving post-embedding of CDs into MOF surfaces or pores, and a one-pot hydrothermal method in which CDs served as nucleation centers for MOF growth. Different synthesis strategies led to either red- or blue-shifted emission of CDs. By blending these two CDs@MOFs as emissive layers in LEDs and adjusting their ratios, tunable white LEDs ranging from cool white to warm white were achieved [94]. Notably, the fluorescence intensity of the LEDs remained nearly constant as the temperature increased from 30 to 90 ° C, indicating excellent thermal stability (**Figure 9c**). Owing to their continuously tunable emission spectra and outstanding photostability, CDs@MOFs have also been explored for plant-growth lighting. By inserting red-emissive CDs into the pores of mesoporous MOFs under heated stirring conditions, Zhang et al. fabricated CDs@MOFs and successfully constructed far-red (FR) LEDs. Comparative cultivation experiments with commercial plant lamps revealed that, after 14 days, lettuce seedlings grown under both light sources showed similar morphology, while those illuminated by the FR-LEDs exhibited increased fresh and dry weights, along with significantly enhanced chlorophyll and soluble protein contents [95]. These results demonstrate that FR-LEDs plant growth lamps based on CDs@MOFs can effectively enhance biomass accumulation owing to their optimized emission characteristics (**Figure 9d**).

5.2 Therapy

CDs@MOFs composites integrate the outstanding optical properties and biocompatibility of CDs with the structurally

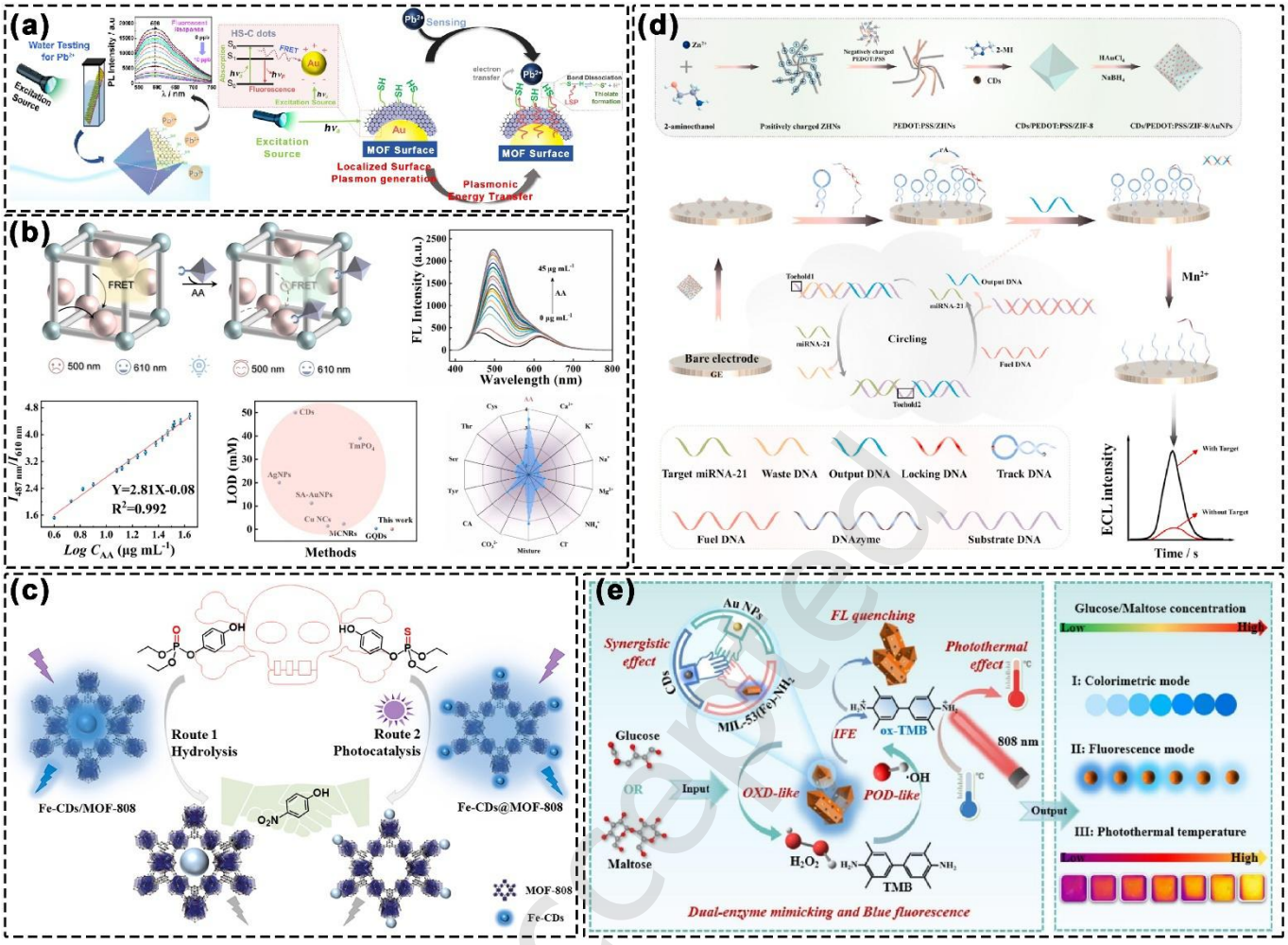

Figure 11. Sensing application of CDs@MOFs. (a) Lead ion detection. Reproduced with permission from Ref. [119], Copyright American Chemical Society, 2022. (b) Ascorbic acid molecular detection. Reproduced with permission from Ref. [120], Copyright Elsevier, 2026. (c) Organophosphorus pesticide detection. Reproduced with permission from Ref. [121], Copyright Elsevier, 2023. (d) Electrochemiluminescence detection. Reproduced with permission from Ref. [124], Copyright Elsevier, 2024. (e) Multi-mode synergistic detection. Reproduced with permission from Ref. [125], Copyright Elsevier, 2025.

tunable porosity and functional metal ions of MOFs, offering broad prospects in biomedical therapy [96]. The therapeutic efficacy of these systems relies on precise regulation of the pathological microenvironment, including infection suppression, modulation of oxidative stress, activation of specific cell death pathways, and light-responsive treatments [97]. MOFs serves as an efficient platform for the storage and controlled release of drugs, metal ions, or bioactive species, while their metal ions (e.g., Zn^{2+}, Cu^{2+}, or Fe^{2+}) can directly participate in biological regulation [98]. Meanwhile, CDs exhibit antioxidant activity, photothermal conversion, or reactive oxygen species (ROS) generation under light irradiation or microenvironmental stimuli, enabling synergistic multimodal therapeutic effects [99-101]. In wound healing applications, CDs@MOFs composites accelerate tissue repair through antibacterial and anti-inflammatory activities, oxidative stress regulation, and angiogenesis promotion. For example, CDs were embedded into MOF constructed via coordination between Fe^{3+} and carboxybenzyl penicillin (CARB), followed by immobilization on cellulose nonwoven fabric to fabricate a smart composite dressing. Under infection-induced acidic conditions, the dressing simultaneously restored fluorescence and released CARB, enabling real-time infection monitoring and effective antibacterial therapy. As infection subsided, reduced bacterial activity led to a local pH increase, which in turn decreased CARB release through a pH-responsive negative feedback mechanism [102]. Additionally, Fe^{3+} competitively coordinated with bacterial ligands and CDs, coupling sensing and therapy. In a murine wound model, this dressing significantly accelerated wound closure, suppressed bacterial proliferation, and allowed visualization of infection severity (**Figure 10a**). Similarly, a nanozyme-integrated MOF was constructed using CDs as ligands and Zn^{2+} as the central metal. CDs exhibited oxidase-like activity, protecting biological systems from ROS-induced damage, while Zn^{2+} provided intrinsic antibacterial functionality. This integration strategy prevented nanozyme aggregation, improved biocompatibility, and enabled tunable release of CDs and Zn^{2+}. In vivo studies demonstrated that the CDs@MOFs effectively alleviated inflammation at diabetic wound sites, promoted angiogenesis, enhanced collagen deposition, and facilitated tissue remodeling [103]. By integrating sonosensitizing CDs and calcium peroxide into

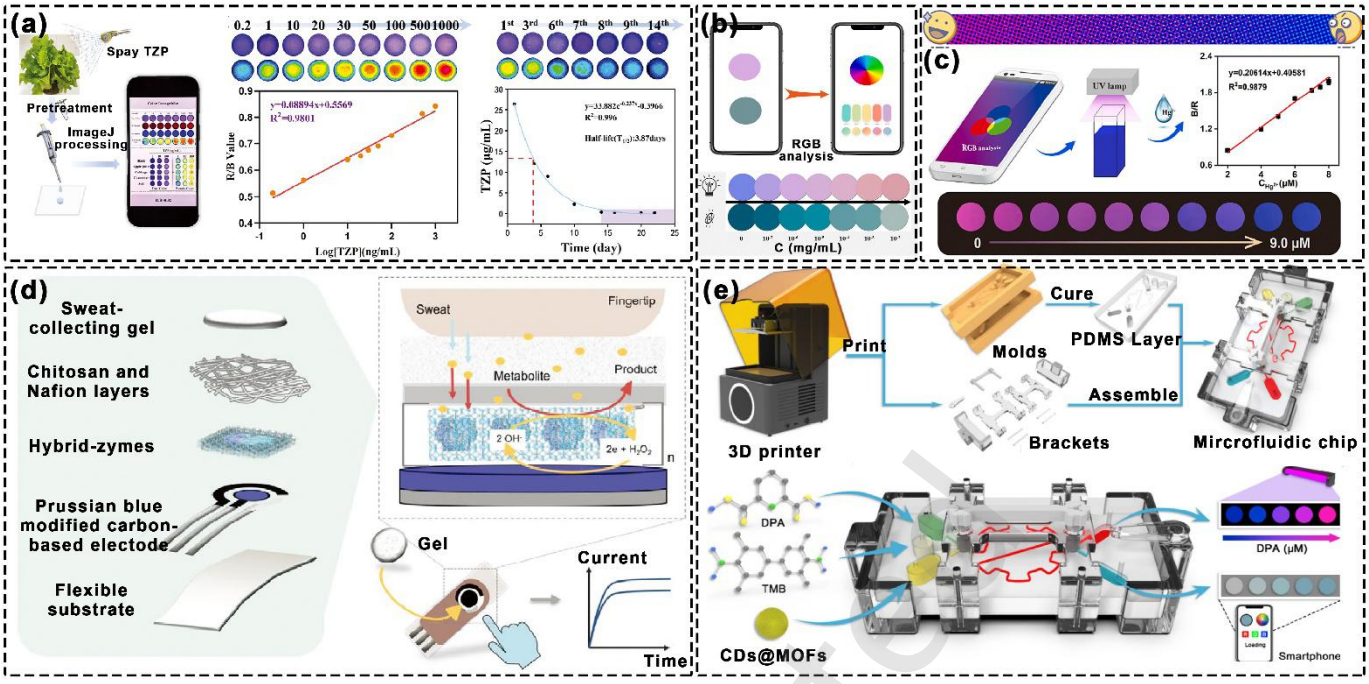

Figure 12. Device integration and portable sensing of CDs@MOFs. (a) Ratio fluorescence detection platform. Reproduced with permission from Ref. [129], Copyright Wiley, 2025. (b) RGB color recognition. Reproduced with permission from Ref. [130], Copyright Elsevier, 2025. (c) RGB linear recognition. Reproduced with permission from Ref. [131], Copyright Elsevier, 2024. (d) Wearable sensors. Reproduced with permission from Ref. [132], Copyright Wiley, 2024. (e) Microfluidic chips integrated into wearable devices. Reproduced with permission from Ref. [133], Copyright Springer, 2025.

MOFs, CDs@MOFs system was developed for immunotherapy via synergistic induction of cuproptosis, ferroptosis, and Ca^{2+} overload. The CDs@MOFs induced ferroptosis accompanied by intracellular glutathione (GSH) depletion and lipid peroxidation accumulation. Concurrently, excessive Cu^{2+} released from the system promoted aggregation of lipoylated dihydrolipoamide S-acetyltransferase, further triggering cuproptosis [104]. Under ultrasound irradiation, the sonosensitizing CDs generated ROS, amplifying oxidative stress and activating antitumor immune responses (**Figure 10b**). To achieve tumor-specific drug release, Shen et al. employed CDs to protect a doxorubicin (DOX)-loaded MOFs from degradation under physiological conditions [105]. The resulting DOX-CDs@MOF selectively degraded in the acidic tumor microenvironment, releasing CDs and DOX to trigger tumor-specific ferroptosis and chemotherapy. A single treatment was sufficient to eradicate tumors via tumor-targeted chemotherapy combined with enhanced ferroptosis-mediated sonodynamic and chemodynamic therapy. In photothermal and photodynamic therapy, CDs serve as efficient photoresponsive units, while MOFs confine and enrich photosensitizers and oxygen, significantly improving therapeutic efficiency and reducing side effects (**Figure 10c**). Jin et al. reported the CDs@MOFs responsive to both the tumor microenvironment and near-infrared light, which decomposed endogenous H_2O_2 via Fenton-like reactions. The system exhibited pronounced NIR photothermal therapy effects and depleted GSH, thereby enhancing H_2O_2 decomposition and increasing intracellular ROS levels, ultimately improving the efficacy of photodynamic therapy and chemodynamic therapy. Similarly, a self-assembled CDs@MOFs was synthesized using CDs, $FeCl_3$, and trimesic acid as precursors [106]. Upon entering the tumor microenvironment, elevated GSH levels reduced Fe^{3+} to Fe^{2+} while consuming GSH, leading to framework disintegration and release of CDs and Fe^{2+}. Fluorescence from CDs was restored and switched "on," enabling tumor imaging. Meanwhile, the released Fe^{2+} reacted with H_2O_2 via the Fenton reaction to generate highly reactive hydroxyl radicals (•OH), achieving chemodynamic therapy. Consequently, under fluorescence imaging guidance, an efficient tumor microenvironment-responsive synergistic chemodynamic-photothermal therapeutic strategy was realized (**Figure 10d**).

5.3 Sensing

CDs@MOFs composites exhibit broad application potential in sensing owing to their excellent optical responsiveness and highly designable porous architectures [107-109]. The fundamental sensing mechanism relies on analyte – material interactions that induce measurable changes in optical, electrical, or chemical signals [110, 111]. The well-defined pore channels and abundant coordination sites of MOFs enable selective enrichment and recognition of target species, including metal ions, small molecules, and pesticides [112, 113]. CDs serve as highly sensitive signal transduction units, whose fluorescence intensity, emission wavelength, or lifetime can respond rapidly to microenvironmental variations [114-116]. In the detection of metal ions (e.g., Fe^{3+}, Hg^{2+}, and Cu^{2+}), organic molecules, and pesticides, CDs@MOFs typically achieve high sensitivity through coordination interactions, static or dynamic fluorescence quenching, inner filter effects, or energy transfer mechanisms [117 118]. By mimicking metal–protein

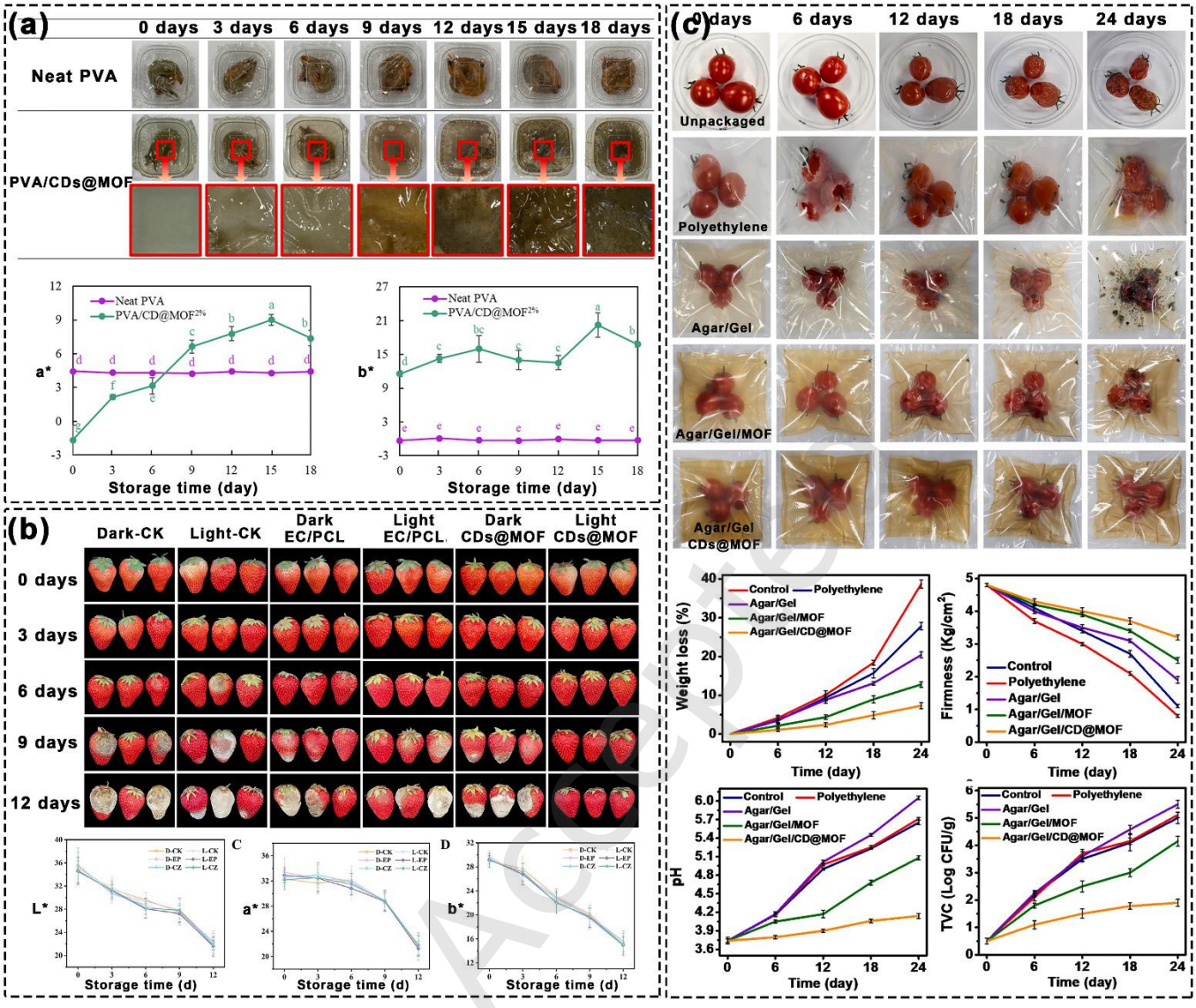

Figure 13. Food Preservation of CDs@MOFs. (a) Shrimp freshness observation. Reproduced with permission from Ref. [138], Copyright Elsevier, 2025. (b) Strawberry preservation. Reproduced with permission from Ref. [139], Copyright Wiley, 2025. (c) Tomato preservation. Reproduced with permission from Ref. [140], Copyright Elsevier, 2024.

interactions in biological systems, Doherty et al. developed a biomimetic CDs@MOFs capable of highly sensitive and selective detection of Pb^{2+}. The CDs@MOFs film containing 1.4 wt% gold exhibited a pronounced quenching response, achieving a detection limit as low as 800 ppt while maintaining stable performance over five sensing cycles (**Figure 11a**) [119]. Song et al. encapsulated CDs into MOFs to construct a ratiometric luminescent CDs@MOFs probe for the selective recognition and sensitive detection of ascorbic acid (AA). Upon interaction with AA, the absorption peak at 550 nm decreased significantly, attributed to the formation of a binary complex between CDs and AA, which altered the absorption characteristics of CDs at this wavelength. During sensing, a distinct fluorescence color transition from orange-red to yellow and then to green was observed with the naked eye. The probe exhibited a linear detection range of 0.02 – 255 μM and a detection limit of 6.6 nM. (**Figure 11b**) [120]. Zhang et al. integrated CDs with MOF-808 to achieve selective degradation and sensitive detection of paraoxon and parathion. Two distinct CDs@MOFs composites were synthesized via host-guest interactions. The fluorescence of the nanocomposites was quenched by the inner filter effect of the organophosphate degradation product 4-nitrophenol [121]. The CDs/MOFs exhibited a linear detection range of 0.001 – 360 μM for paraoxon with a detection limit of 0.3 nM, while CDs@MOFs showed a linear range of 0.01-100 μM for parathion with a detection limit of approximately 3.3 nM. The composites were further applied to the analysis of organophosphate residues in real samples, where detection results in pak choi were consistent with those obtained by high-performance liquid chromatography (**Figure 11c**). Beyond fluorescence-based sensing, electrochemiluminescence (ECL) biosensing systems have also demonstrated significant potential [122, 123]. Wang et al. constructed CDs@MOFs using CDs as luminophores and ZIF-8 as a carrier, with PEDOT: PSS introduced to enhance electrical conductivity, resulting in substantially improved luminescence performance. Further modification with gold nanoparticles led to an approximately tenfold enhancement factor compared with individual CDs [124]. Coupled with a

DNAzyme-based dual-cycle target amplification strategy, an ECL biosensor was developed for highly sensitive detection of miRNA-21, achieving a detection limit as low as 50 aM (**Figure 11d**). In addition to single-mode sensing, Li et al. realized multimodal detection of glucose and maltose based on colorimetric, fluorescence, and photothermal responses [125]. The CDs@MOFs functioned simultaneously as a fluorescent probe, an oxidase-mimicking nanozyme generating H_2O_2, and a peroxidase-mimicking catalyst producing •OH radicals, yielding low detection limits of 12, 7.5, and 1.1 μM, respectively (**Figure 11e**).

In terms of sensor device integration, CDs@MOFs composites can be incorporated into thin films, paper-based substrates, or microstructured platforms to construct portable and visually readable sensing systems [126]. Their stable fluorescence signals can be captured using smartphone cameras or portable light sources, enabling quantitative analysis of color or intensity variations and thereby facilitating the transition of laboratory-based sensing technologies toward rapid on-site detection [127, 128]. Li et al. encapsulated CDs within the internal cavities of Au-ZIF to synthesize CDsMOFs to monitor the degradation of triazophos (TZP) sprayed onto lettuce leaves using a hydrogel-based sensor [129]. A fitting equation was established within the lettuce matrix to accurately track TZP degradation over time. Combined with image-processing algorithms, quantitative detection was achieved with a detection limit as low as 0.07 ng mL^{-1} (**Figure 12a**). RGB color recognition represents one of the most widely adopted intelligent detection modes. During sensing, a smartphone equipped with a self-developed color-recognition application converts colorimetric and fluorescence images into RGB values, enabling quantitative analysis through simple color variations and providing a practical reference for rapid on-site semi-quantitative detection. As shown in **Figure 12b**, when the analyte concentration increased from 10^{-7} to 10^{-2} mg mL^{-1}, the blue channel in the colorimetric mode gradually faded [130]. In another example, the color information in photographs was converted into RGB values using a smartphone-based color detector to determine analyte concentrations (**Figure 12c**) [131]. Beyond portable detection, CDs@MOFs can also be employed to construct flexible and wearable sensors for real-time monitoring of environmental or physiological signals [132]. By incorporating CDs@MOFs into flexible substrates, Yang et al. demonstrated a touch-based glucose sensor prototype capable of continuously monitoring glucose levels in fingertip sweat for one month at room temperature, while maintaining excellent electrochemical sensitivity after storage at physiological temperature for 30 days (**Figure 12d**). Furthermore, Zhang et al. developed a 3D-printed microfluidic chip for on-chip dual-mode detection of DPA, integrating both ratiometric fluorescence and colorimetric sensing [133]. To enhance usability and minimize environmental or instrumental variability, the microfluidic chip was integrated into a semi-portable device and operated via smartphone control, resulting in a compact and user-friendly system. Under smartphone-assisted operation, detection limits derived from RGB signal analysis were 0.33 μM and 12.27 μM, respectively (**Figure 12e**).

5.4 Food Preservation

Foods are prone to quality deterioration during storage due to microbial proliferation, oxidative reactions, and the accumulation of gaseous byproducts [134]. By integrating the optical and chemical functionalities of CDs with the structural advantages of MOFs, CDs@MOFs offer a multifunctional and synergistic strategy for the preservation of meat, fruits, and vegetables [135]. On the one hand, the high specific surface area and tunable pore structures of MOFs enable efficient adsorption of oxygen, carbon dioxide, and ethylene, among which ethylene capture is particularly critical for significantly delaying the ripening and senescence of fruits and vegetables [136]. On the other hand, the antibacterial and antioxidant activities exhibited by CDs and certain MOFs metal ions effectively suppress microbial growth on food surfaces and mitigate lipid oxidation, discoloration, and nutrient loss [137]. Kim et al. employed PVA-coated CDs@MOFs film for food preservation studies, in which the film color gradually changed from green to brown with increasing storage time. In contrast, pure PVA films exhibited negligible changes in the a* and b* values during shrimp spoilage [138]. The pronounced color transition observed in the CDs@MOFs films arises from the pH sensitivity of both CDs and MOFs. Specifically, protonation or deprotonation of surface functional groups on CDs alters their electronic structure in response to pH variations, resulting in distinct color changes. Similarly, MOF structures are sensitive to pH fluctuations, which modify the metal–ligand coordination environment and consequently affect their optical properties. The synergistic interaction between CDs and MOFs amplifies the colorimetric response, producing a clear transition from green to brown as shrimp spoilage progresses. This pH-responsive behavior provides a reliable visual indicator for real-time monitoring of shrimp freshness (**Figure 13a**). CDs@MOFs nanofibrous membranes exhibit pronounced photodynamic antibacterial activity, favorable biosafety, and excellent physicochemical properties, rendering them highly promising for strawberry preservation. As shown in **Figure 13b**, no significant differences in appearance were observed among the strawberry groups during the first three days of storage. In the control group, partial spoilage and deterioration became evident by day 6, and severe decay occurred between days 9 and 12, rendering the fruit unsuitable for consumption [139]. In contrast, strawberries treated with CDs@MOFs nanofibrous membranes under photodynamic conditions maintained good quality without visible spoilage even after 12 days of storage. Colorimetric analysis using a color difference meter revealed no significant differences in color parameters among the treatment groups (**Figure 13b**). During 24 days of storage at 4 °C, Kim et al. monitored the physicochemical and microbiological parameters of tomatoes subjected to different packaging treatments [140]. Tomatoes in the control group, polyethylene packaging, and agar/gel packaging exhibited rapid increases in visible damage and mold growth. In comparison, agar/gel/MOF composite films significantly reduced the degradation rate of packaged tomatoes. Notably, tomatoes packaged with agar/gel/CDs@MOFs films showed negligible visible decay, indicating the effectiveness of the designed nanocomposite

films in extending tomato shelf life. Although weight changes were observed in all groups during storage, the control group exhibited more pronounced weight loss than the agar/gel/CDs@MOFs-packaged group. Weight loss in fresh fruits during storage is primarily attributed to respiratory activity and moisture evaporation, leading to water loss (**Figure 13c**).

6 Conclusions

This review systematically summarize the construction strategies, structural characteristics, luminescence regulation mechanisms, and recent research progress of CDs@MOFs composites in applications including sensing, anti-counterfeiting, lighting and display, food preservation, and biotherapy. By integrating CDs with metal – organic framework materials, the confinement effect, rigid skeleton, and highly designable microenvironments of MOFs offer distinct advantages for the precise regulation of carbon dot luminescence. These features not only effectively suppress aggregation-induced quenching under solid-state conditions but also enable luminescence enhancement, solid-state emission, activation of room-temperature phosphorescence, and multimodal optical responses. Meanwhile, diverse synthetic routes and integration modes endow CDs@MOFs systems with excellent structural tunability and functional integration capability, positioning them as an important platform for the development of next-generation carbon-based functional materials. Despite the significant advances achieved in recent years, the CDs@MOFs field still faces several critical scientific and technological challenges.

(1) Interfacial structure regulation of CDs@MOFs composites

Although substantial progress has been made in exploiting the confinement effect and rigid frameworks of MOFs to modulate the luminescence of CDs, a comprehensive understanding of the true interfacial binding modes, structural configurations, and their impacts on energy-level alignment and excited-state dynamics remains elusive. Most existing studies rely on indirect spectroscopic evidence to interpret emission enhancement or phosphorescence activation, while the microscopic origins of charge/energy transfer pathways, singlet–triplet conversion, and interfacial electronic coupling are still insufficiently resolved. Future investigations should integrate in situ and time-resolved characterization techniques (such as ultrafast transient absorption spectroscopy, in situ photoluminescence, EPR, and X-ray absorption spectroscopy) with first-principles calculations and excited-state simulations. Such combined experimental – theoretical approaches will be essential for establishing a clear structure – property – dynamics relationship and enabling the rational design of CDs@MOF systems with predictable and tunable photophysical behaviors.

(2) Device-level translation of CDs@MOFs

Despite their promising optical performance and multifunctionality, the application of CDs@MOF composites in device-level systems, including light-emitting diodes, sensing platforms, and flexible wearable electronics, remains at an early developmental stage. Critical issues such as structural optimization, long-term operational stability, and scalable fabrication have not yet been sufficiently addressed. Future research should focus on evaluating the performance of CDs@MOF-based devices under practical operating conditions, thereby accelerating the transition of CDs@MOF materials from laboratory-scale demonstrations to reliable and practical optoelectronic and sensing devices.

(3) Safety, stability, and degradability in biomedical and food-related applications

In biomedical and food-related applications, CDs@MOF composites have demonstrated considerable potential in imaging, therapy, preservation, and quality monitoring. However, systematic evaluations of biosafety, environmental stability, and biodegradability remain insufficient. Most current studies emphasize functional performance, whereas the long-term behavior of these composites in complex biological environments or food storage conditions is less explored. Future efforts should incorporate comprehensive toxicological assessments, in vivo metabolism studies, and environmental degradation analyses to clarify the fate and potential risks associated with MOF metal nodes, organic ligands, and CDs during use and disposal. Furthermore, the design of low-toxicity, biodegradable, and biofriendly MOF frameworks, in combination with green and sustainable carbon-dot synthesis routes, will be crucial for improving the translational feasibility and regulatory acceptance of CDs@MOF materials in biomedical and food safety applications.

(4) Standardization, scalability, and practical deployment of CDs@MOFs

Despite the rapid development of CDs@MOF composites, their transition toward practical applications is still hindered by the lack of standardized evaluation protocols and scalable fabrication strategies. One key challenge lies in the reproducibility of composite structures, as variations in CDs size, surface states, and MOF crystallization conditions can lead to significant batch-to-batch differences in optical and functional performance. Establishing standardized synthesis procedures, along with unified metrics for evaluating luminescence efficiency, stability, and sensing performance, will be essential for comparing results across different studies.

Data availability

Not applicable.

Acknowledgements

This work was supported by the National Natural Science Foundation of China (Nos. U24A2079) and the foundation of scientific research project of colleges and universities in Anhui Province (2025AHGXZK40130).

Declaration of competing interest

All the contributing authors report no conflict of interests in this work.

Author contribution statement

B. W.: Writing manuscript, investigation, validation, formal analysis, software. N. Q.: Writing manuscript, investigation, project administration. S. L.: Funding acquisitionm, resources, investigation, writing editing, supervision, validation. All the authors have approved the final manuscript.

Use of AI statement

None.

References

[1] Zhou, H.; Kim, H.-W.; Han, S. J.; Zhang, D.; Jeong, W. J.; Yu, H.; Tsuchiya, Y.; Hu, B.; Huh, J.; Zhang, T.; et al. Exciplex-enabled high-efficiency, fully stretchable OLEDs. *Nature* **2026**, *649* (8097), 604–611.

[2] Zeng, Q.; Zhao, Y.; Park, S.; Zhou, H.; Shim, H.-J.; Li, T.; Ryu, J.; Sung, M.-J.; Chua, X. W.; Yoon, E.; et al. A hierarchical shell locks and stabilizes perovskite nanocrystals with near-unity quantum yield. *Science* **2026**, *391* (6782), eady1370.

[3] Adrover, J. M.; Han, X.; Sun, L.; Fujii, T.; Sivetz, N.; Daßler-Plenker, J.; Evans, C.; Peters, J.; He, X.-Y.; Cannon, C. D.; et al. Neutrophils drive vascular occlusion, tumour necrosis and metastasis. *Nature* **2025**, *645* (8080), 484–495.

[4] Groessl, S.; Kalis, R.; Snaebjornsson, M. T.; Wambach, L.; Haider, J.; Andersch, F.; Schulze, A.; Palm, W.; Zuber, J. Acidosis orchestrates adaptations of energy metabolism in tumors. *Science* **2025**, *390* (6769), eadp7603.

[5] Zou, C.; Ren, Z.; Hui, K.; Wang, Z.; Fan, Y.; Yang, Y.; Yuan, B.; Zhao, B.; Di, D. Electrically driven lasing from a dual-cavity perovskite device. *Nature* **2025**, *645* (8080), 369–374.

[6] Lan, Y.; Li, S.; Guo, H.; Liu, Q.; Wang, T.; Zhou, L.; Fang, J.; Zhao, Y.; Zhou, Z.; Wang, Q.; et al. Soft biodegradable implants for long-distance and wide-angle sensing. *Nature* **2026**, *649* (8096), 366–374.

[7] Liang, Y.; Chen, G.; Wang, Y.; Zou, Y.; Feng, M.; Wang, Y.; Li, B.; Cho, Y.; Chang, Y.; Liu, T.; et al. A matrix-confined molecular layer for perovskite photovoltaic modules. *Nature* **2025**, *648* (8092), 91 – 96.

[8] Đorđević, L.; Arcudi, F.; Cacioppo, M.; Prato, M. A multifunctional chemical toolbox to engineer carbon dots for biomedical and energy applications. *Nat. Nanotechnol.* **2022**, *17* (2), 112–130.

[9] Xie, W.; Wang, H.; Xu, H.; Su, W.; Yuan, T.; Chang, J.; Bai, Y.; Fan, Y.; Zhang, Y.; Li, Y.; et al. Sterically chained amino acid-rich water-soluble carbon quantum dots as a robust tumor-targeted drug delivery platform. *Nat. Commun.* **2025**, *16* (1), 2716.

[10] Zhang, T.; Cheng, Q.; Cheng, H.; Wang, Q.; Wang, B.; Zhang, B.; Sun, H.; Deng, C.; Tang, Z. Manipulation of magnetic edge states in carbon quantum dots for magnetic resonance imaging and NIR-II photo-thermoelectric therapy. *Nat. Commun.* **2025**, *16* (1), 5867.

[11] Wang, B.; Waterhouse, G. I. N.; Yang, B.; Lu, S. Advances in Shell and Core Engineering of Carbonized Polymer Dots for Enhanced Applications. *Acc. Chem. Res.* **2024**, *57* (19), 2928–2939.

[12] Zhang, Y.; Zeng, X.; Wen, X.; Ding, S.; Yang, Y.; Hu, Y.; Lu, S. Current status and future prospects of non-toxicity carbon-dot-based miniaturized lasers. *Natl. Sci. Rev.* **2025**, *12* (11), nwaf426.

[13] Song, H.; Ru, Y.; Yu, J.; Tao, S.; Li, Y.; Liu, H.; Liu, Y.; Zhang, H.; Wu, H.; Cheng, Y.; et al. Carbon dots: from fundamentals to frontier applications. *Sci. China Chem.* **2026**, *69*, 539–618.

[14] Wang, B.; Wang, J.; Lu, S. Carbon Dots: Small Materials With Big Impacts on Optoelectronic Devices. *Aggregate* **2025**, *6* (12), e70212.

[15] Tao, S.; Zheng, C.; Yang, B. Precursor-dependent photoluminescence diversity in carbonized polymer dots: the luminophores and crosslinking. *Natl. Sci. Rev.* **2025**, *12* (10), nwaf377.

[16] Wang, B.; Lu, S. The light of carbon dots: From mechanism to applications. *Matter* **2022**, *5* (1), 110–149.

[17] Li, X.; Chen, K.; Guo, R.; Wei, Z. Ionic Liquids Functionalized MOFs for Adsorption. *Chem. Rev.* **2023**, *123* (16), 10432–10467.

[18] Khalil, I. E.; Fonseca, J.; Reithofer, M. R.; Eder, T.; Chin, J. M. Tackling orientation of metal-organic frameworks (MOFs): The quest to enhance MOF performance. *Coordin. Chem. Rev.* **2023**, *481*, 215043.

[19] Wang, W.; Chen, D.; Li, F.; Xiao, X.; Xu, Q. Metal-organic-framework-based materials as platforms for energy applications. *Chem* **2024**, *10* (1), 86–133.

[20] Yuan, Y.; Jia, H.; Liu, J.; Gao, F.; Zhu, X.; An, Z.; Wang, J. Application of microfluidic chip coupled with carbon dots-MOF-enriched chromogenic membrane in the detection of various perfluorinated compounds. *J. Hazard. Mater.* **2026**, *504*, 141245.

[21] Ali, K.; Sethi, P.; Basu, S. ZIF-67/CQD nanohybrids for combined adsorptive and photocatalytic removal of tetracycline: kinetic, isotherm, and mechanistic insights. *RSC Sustainability* **2026**, *4* (3), 1436–1455.

[22] Brito, T. P.; Llanos, L.; Singh, D. P. Carbon dots and metal–organic frameworks based nanohybrids for improved biosensing and biomedical applications. *Nanoscale Adv.* **2026**, *8* (5), 1450–1489.

[23] Hammad, S. F.; Abdallah, I. A.; Bedair, A.; Abdelhameed, R. M.; Locatelli, M.; Mansour, F. R. Metal organic framework-derived carbon nanomaterials and MOF hybrids for chemical sensing. *TrAC Trend. Anal. Chem.* **2024**, *170*, 117425.

[24] Barcus, K.; Cleveland, J. M.; Gudi, D.; Bennett, K. J.; Thon, S. M.; Thoi, V. S. Charge transfer in hybrid quantum dot / metal-organic framework systems: Current understanding and future challenges. *Coordin. Chem. Rev.* **2025**, *542*, 216841.

[25] Bazazi, S.; Hashemi, E.; Mohammadjavadi, M.; Saeb, M. R.; Liu, Y.; Huang, Y.; Xiao, H.; Seidi, F. Metal-organic framework (MOF)/C-dots and covalent organic framework (COF)/C-dots hybrid nanocomposites: Fabrications and applications in sensing, medical, environmental, and energy sectors. *Adv. Colloid Interf. Sci.* **2024**, *328*, 103178.

[26] Ye, Z.; Bao, Y.; Chen, Z.; Ye, H.; Feng, Z.; Li, Y.; Zeng, Y.; Pan, Z.; Ouyang, D.; Zhang, K.; et al. Recent advances in the metal/organic hybrid nanomaterials for cancer theranostics. *Coordin. Chem. Rev.* **2024**, *504*, 215654.

[27] Liu, S.-Z.-Y.; Lou, Q.; Hu, Y.-S.; Shan, C.-X. Carbon dot-based lasing systems: A review of material synthesis, device architectures, and performance optimization. *Nano Res.* **2025**, *18* (8), 94907606.

[28] Li, W.; Yue, D.; Liu, Y.; Li, Y.; Zhang, B.; Qin, B.; Zhang, Y.; Wang, Z.; Lu, S. Rare earth-carbon dots hybrids: a critical review of synthetic pathways, energy transfer mechanisms, and advanced photonic applications. *Coordin. Chem. Rev.* **2026**, *558*, 217775.

[29] Yu, H.; Ai, L.; Lu, S. Second near-infrared fluorophores: Rational design, optical enhancement strategies, and recent advances in imaging-guided biomedical applications. *Chem* **2026**, *12* (3), 102867.

[30] Zhao, C.; Tian, Y.; Li, C.; Sheng, X. Recent advances in the use of carbon dots in polymer coatings: a prospective review. *Nanoscale* **2026**, *18* (6), 2889–2915.

[31] Latiza, R. J. P.; Olay, J.; Eguico, C.; Yan, R. J.; Rubi, R. V. Surface matters: passivation in carbon dot synthesis—a critical review. *J. Mater. Sci.* **2025**, *60* (11), 5006–5018.

[32] Mohammed, A. S.; Mohammed, S. J. Carbon dot-integrated edible films: emerging synergies for advanced food packaging applications. *RSC Adv.* **2026**, *16* (13), 12012–12036.

[33] Yang, X.-C.; Fu, S.-Q.; Li, Q.-L.; Jiao, Z.; Zhao, J.-T.; Guo, Y.; Zhang, Z.-J.; Gao, S.; Cheng, L.-L. Superior triethylamine sensing platform based on MOF activated by carbon dots for photoelectric dual-mode in biphasic system. *Chem. Eng. J.* **2023**, *465*, 142869.

[34] Rehman, T. U.; Agnello, S.; Gelardi, F. M.; Madonia, A.; Sciortino, A.; Calvino, M. M.; Lazzara, G.; Minervini, G.; Panniello, A.; Buscarino, G.; et al. Engineering MIL-53(Al) MOF with Carbon Dots for Synergistic Photocatalysis Applications in Organic Dye Degradation. *ACS Omega* **2025**, *10* (18), 18527–18538.

[35] Zhang, J.; Liu, Y.; Cui, X.; Cao, Y.; Li, Y.; Fang, G.; Wang, S. A Smartphone-Integrated Molecularly Imprinted Fluorescence Sensor for Visual Detection of Chlortetracycline Based on N,P-Codoped Carbon Dots Decorated Iron-Based Metal–Organic Frameworks. *J. Agric. Food Chem.* **2023**, *71* (43), 16303–16309.

[36] Hu, X.; Cao, Y.; Cai, L.; Wang, H.; Fang, G.; Wang, S. A smartphone-assisted optosensing platform based on chromium-based metal-organic framework signal amplification for ultrasensitive and real-time determination of oxytetracycline. *J. Hazard. Mater.* **2023**, *444*, 130395.

[37] Yang, J.; Cheng, Q.; Zhu, C. C.; Huang, H. Y.; Su, J. B.; Ni, W.; Ruan, B.; Ma, N.; Tsai, F. C. Folic acid conjugated carbon dots doped metal-organic framework materials for cell imaging. *Mater. Today Chem.* **2022**, *26*, 101202.

[38] Zou, Y.; Weng, J.; Qin, Z.; Zhang, Y.; Ji, S.; Zhang, H. Metal–organic framework- and graphene quantum dot-incorporated nanofibers as dual stimuli-responsive platforms for day/night antibacterial bio-protection. *Chem. Eng. J.* **2023**, *473*, 145365.
[39] Wu, S.; Chen, C.; Chen, J.; Li, W.; Sun, M.; Zhuang, J.; Lin, J.; Liu, Y.; Xu, H.; Zheng, M.; et al. Construction of carbon dots/metal–organic framework composite for ratiometric sensing of norfloxacin. *J. Mater. Chem. C* **2022**, *10* (41), 15508–15515.
[40] Zhao, D. L.; Jin, H.; Zhao, Q.; Xu, Y.; Shen, L.; Lin, H.; Chung, T.-S. Smart integration of MOFs and CQDs to fabricate defect-free and self-cleaning TFN membranes for dye removal. *J. Membrane Sci.* **2023**, *679*, 121706.
[41] Qu, M.; Yu, H.; He, Y.; Xu, W.; Liu, D.; Cheng, F. Ce-UiO-66-F4-based composites decorated with green carbon dots for universal adsorption of organic pollutants containing hydrogen bond donors and its application exploration. *Chem. Eng. J.* **2024**, *486*, 150266.
[42] Pan, M.; Sun, J.; Wang, Y.; Yang, J.; Wang, Z.; Li, L.; Wang, S. Carbon-dots encapsulated luminescent metal–organic frameworks@surface molecularly imprinted polymer: A facile fluorescent probe for the determination of chloramphenicol. *Food Chem.* **2024**, *442*, 138461.
[43] Yang, Q.; Hong, H.; Luo, Y. Heterogeneous nucleation and synthesis of carbon dots hybrid Zr-based MOFs for simultaneous recognition and effective removal of tetracycline. *Chem. Eng. J.* **2020**, *392*, 123680.
[44] Wang, D.; Zhao, Z.; Shi, B.; Wang, J.-X.; Chen, J.-F. Real-Time Imaging and Quantitative Evolution for Pyrolysis of Carbon Dots-Encapsulated Metal–Organic Frameworks at the Nanoscale by In Situ Environmental Transmission Electron Microscopy. *ACS Appl. Mater. Interfaces* **2023**, *15* (29), 35358–35365.
[45] Xia, Z.; Shi, B.; Zhu, W.; Lü, C. Temperature-responsive polymer-tethered Zr-porphyrin MOFs encapsulated carbon dot nanohybrids with boosted visible-light photodegradation for organic contaminants in water. *Chem. Eng. J.* **2021**, *426*, 131794.
[46] Peng, L.; Guo, H.; Ren, B.; Hui, Y.; Zhuang, D.; Liu, Y.; Yan, R.; Niu, W.; Yang, W. A novel dual-function fluorescence sensor Eu/CDs@MOF-808 for the sensitive detection of adenosine triphosphate and uric acid. *Chem. Eng. J.* **2024**, *500*, 156811.
[47] Li, Y.; Huang, K.; Liu, W.; Wang, K.; Fu, S.; Guo, H.; Zhang, J.; Lian, C.; Wang, L. Interfacial engineering of carbon quantum dot/metal-organic framework heterostructures for boosted urea electrosynthesis from carbon dioxide and nitrate. *J. Colloid Interf. Sci.* **2026**, *703*, 139264.
[48] Hedau, B.; Park, S.-J.; Kang, B.-C.; Ha, T.-J. Bifunctional carbon quantum dot-embedded metal-organic framework nanohybrid as a highly efficient electrocatalyst for water splitting and CO2 reduction. *Carbon* **2024**, *216*, 118527.
[49] Wiwasuku, T.; Suebphanpho, J.; Ittisanronnachai, S.; Promarak, V.; Boonmak, J.; Youngme, S. Nanoscale carbon dot-embedded metal–organic framework for turn-on fluorescence detection of water in organic solvents. *RSC Adv.* **2023**, *13* (26), 18138–18144.
[50] Zhang, Y.; Cui, X.; Wang, X.; Feng, X.; Deng, Y.; Cheng, W.; Xiong, R.; Huang, C. Xylan derived carbon dots composite ZIF-8 and its immobilized carbon fibers membrane for fluorescence selective detection Cu2+ in real samples. *Chem. Eng. J.* **2023**, *474*, 145804.
[51] Dang, J.; Qiu, J.; Zhang, X.; Jin, R.; Qin, B.; Zhang, J. Nanoflower electrocatalysts derived from mixed metal (Fe/Co/Ni) organic frameworks for the electrochemical oxygen evolution reaction. *CrystEngComm* **2023**, *25* (30), 4299–4305.
[52] Dang, J.; Qiu, J.; Zhang, X.; Zhang, J. Nanosheet arrays derived from ZIF-67 grown on three-dimensional frameworks for the electrocatalytic oxygen evolution reaction. *Dalton Trans.* **2025**, *54* (4), 1468–1475.
[53] Lin, R.; Li, S.; Wang, J.; Xu, J.; Xu, C.; Wang, J.; Li, C.; Li, Z. Facile generation of carbon quantum dots in MIL-53(Fe) particles as localized electron acceptors for enhancing their photocatalytic Cr(vi) reduction. *Inorg. Chem. Front.* **2018**, *5* (12), 3170–3177.
[54] Gu, Z.-G.; Li, D.-J.; Zheng, C.; Kang, Y.; Wöll, C.; Zhang, J. MOF-Templated Synthesis of Ultrasmall Photoluminescent Carbon-Nanodot Arrays for Optical Applications. *Angew. Chem. Int. Ed.* **2017**, *56* (24), 6853–6858.
[55] Meng, X.-B.; Sheng, J.-L.; Tang, H.-L.; Sun, X.-J.; Dong, H.; Zhang, F.-M. Metal-organic framework as nanoreactors to co-incorporate carbon nanodots and CdS quantum dots into the pores for improved H2 evolution without noble-metal cocatalyst. *Appl. Catal. B-Environ. Enery* **2019**, *244*, 340–346.
[56] Hou, Y.; Liu, Z.; Tong, L.; Zhao, L.; Kuang, X.; Kuang, R.; Ju, H. One-step electrodeposition of the MOF@CCQDs/NiF electrode for chiral recognition of tyrosine isomers. *Dalton Trans.* **2020**, *49* (1), 31–34.
[57] Qin, C.; Li, X.; Wang, T.; Xu, Z.; Chen, K.-J.; Pan, F. Metal-Organic Frameworks-Based Copper Catalysts for CO2 Electroreduction Toward Multicarbon Products. *Exploration* **2025**, *5* (3), 270011.
[58] Zhang, Y.; Zhou, H.; Zhao, P.; Yuan, K.; Zhou, R.; Gao, H.; Qu, Y.; Wang, Y. In situ synthesized carbon quantum dots@metal organic framework via corroding Ni foam for efficient oxygen evolution reaction. *Fuel* **2025**, *389*, 134609.
[59] Shatery, O. B. A.; Omer, K. M. Selectivity Enhancement for Uric Acid Detection via In Situ Preparation of Blue Emissive Carbon Dots Entrapped in Chromium Metal–Organic Frameworks. *ACS Omega* **2022**, *7* (19), 16576–16583.
[60] Yao, C.; Xu, Y.; Xia, Z. A carbon dot-encapsulated UiO-type metal organic framework as a multifunctional fluorescent sensor for temperature, metal ion and pH detection. *J. Mater. Chem. C* **2018**, *6* (16), 4396–4399.
[61] Wang, Z.; Jin, X.; Yan, L.; Yang, Y.; Liu, X. Recent research progress in CDs@MOFs composites: fabrication, property modulation, and application. *Microchim. Acta* **2022**, *190* (1), 28.
[62] Lopez, E. C. R.; Perez, J. V. D. Current Advances in the Synthesis of CD-MOFs and Their Water Stability. *Eng. Proc.* **2023**, *56* (1), 72.
[63] Yin, X.; Zhang, Z.; Li, F.; Fu, M.; Qin, T.; Ji, X.; Wang, Y.; Wang, Z.; Sun, S. Applications of Lignin-Dervied Carbon Quantum Dots: Current Status and Challenges. *Exploration* **2025**, *5* (3), 70039.
[64] Yang, J.; Ruan, B.; Ye, Q.; Tsai, L.-C.; Ma, N.; Jiang, T.; Tsai, F.-C. Carbon dots-embedded zinc-based metal-organic framework as a dual-emitting platform for metal cation detection. *Microp Mesopor. Mater.* **2022**, *331*, 111630.
[65] Raufa, A. S. F.; Chi, C.-S.; Chang, C.-W. The Impact of Structural Heterogeneity on the Interpretation of Fluorescence Quenching Mechanisms in Carbon Dots and Carbon Dots@MOF Composites. *J. Phys. Chem. C* **2025**, *129* (47), 20981–20988.
[66] Li, H.-J.; Wang, H.; Si, T.; Wang, H.; Huang, S.; Wu, Y.; Liao, Q.; Wang, D.; Li, Y. Tailoring Morphology and Fluorescence Properties of Zeolitic Imidazolate Frameworks via Carbon Dots. *ACS Appl. Nano Mater.* **2024**, *7* (13), 15535–15546.
[67] Li, J.; Zheng, S.; Zhang, S.; Gong, X. Metal–Organic Framework-Assisted Rational Design of Multicolor Solid-State Fluorescent Carbon Nanodots and Its Application for LEDs. *Laser Photonics Rev.* **2024**, *18* (3), 2300974.
[68] Fu, Q.; Zhang, K.; Lu, K.; Li, N.; Sun, S.; Dong, Z. Recent advances in solid-state fluorescent of red carbon dots: A comprehensive review. *J. Alloy. Compd.* **2024**, *971*, 172688.
[69] Chen, Y.-L.; Kurniawan, D.; Tsai, M.-D.; Chang, J.-W.; Chang, Y.-N.; Yang, S.-C.; Chiang, W.-H.; Kung, C.-W. Two-dimensional metal–organic framework for post-synthetic immobilization of graphene quantum dots for photoluminescent sensing. *Commun. Chem.* **2024**, *7* (1), 108.
[70] Wang, H.; Ai, L.; Song, H.; Song, Z.; Yong, X.; Qu, S.; Lu, S. Innovations in the Solid-State Fluorescence of Carbon Dots: Strategies, Optical Manipulations, and Applications. *Adv. Funct. Mater.* **2023**, *33* (41), 2303756.
[71] Gong, X.; Wu, Y.; Li, J.; Zhang, S.; Wu, M. Rational design of long wavelength solid-state fluorescent carbon dots based on zirconium. *Carbon* **2024**, *226*, 119208.
[72] Yang, X.; Waterhouse, G. I. N.; Lu, S.; Yu, J. Recent advances in the design of afterglow materials: mechanisms, structural regulation strategies and applications. *Chem. Soc. Rev.* **2023**, *52* (22), 8005–8058.
[73] Li, J.; Zhou, H.; Qiu, H.; Yan, Y.; Wang, X.; Gao, Z.; Wang, Z.

Phosphorescent carbon dots: Intermolecular interactions, properties, and applications. *Coordin. Chem. Rev.* **2024**, *503*, 215642.

[74] Zheng, C.; Tao, S.; Yang, B. The Current Progress and Challenges of Carbonized Polymer Dot-Based Room-Temperature Phosphorescent Materials. *CCS Chem.* **2023**, *6* (3), 604–622.

[75] Zhang, L.; Chen, X.; Hu, Y. Pyrolysis of Al-Based Metal–Organic Frameworks to Carbon Dot-Porous Al2O3 Composites With Time-Dependent Phosphorescence Colors for Advanced Information Encryption. *Small* **2024**, *20* (1), 2305185.

[76] Chen, D.; Guo, X.; Sun, X.; Feng, X.; Chen, K.; Zhang, J.; Zhu, Z.; Zhang, X.; Liu, X.; Liu, M.; et al. High-yield upcycling of feather wastes into solid-state ultra-long phosphorescence carbon dots for advanced anticounterfeiting and information encryption. *Exploration* **2024**, *4* (6), 20230166.

[77] Xu, B.; Wang, Z.; Shen, J.; Li, J.; Jia, Y.; Jiang, T.; Gao, Z.; Wang, X.; Meng, X. Metal–Organic Framework-Activated Full-Color Room-Temperature Phosphorescent Carbon Dots with a Wide Range of Tunable Lifetimes for 4D Coding Applications. *J. Phys. Chem. C* **2022**, *126* (28), 11701–11708.

[78] Shi, Y.; Su, W.; Teng, Q.; Li, C.; Yuan, T.; Xu, H.; Song, X.; Han, Y.; Wei, S.; Zhang, Y.; et al. Opportunity and application of chiral carbon dots. *Matter* **2023**, *6* (9), 2776–2806.

[79] Chen, X.; Yu, M.; Li, P.; Xu, C.; Zhang, S.; Wang, Y.; Xing, X. Recent Progress on Chiral Carbon Dots: Synthetic Strategies and Biomedical Applications. *ACS Biomater. Sci. Eng.* **2023**, *9* (10), 5548–5566.

[80] Wang, G.-D.; Wang, X.-Y.; Luo, P.; Dong, X.-Y.; Zhang, C. Multi-responsive CPL switches of carbon dots confined in chiral metal–organic frameworks. *Mater. Chem. Front.* **2025**, *9* (19), 2889–2899.

[81] Wang, X.-Y.; Luo, P.; Dong, X.-Y.; Guan, S.; Zhang, C. Transcription of Customized Circularly Polarized Luminescence from Enantiomeric Metal–Organic Framework to Carbon Dots. *Adv. Optical Mater.* **2024**, *12* (34), 2401713.

[82] Döring, A.; Ushakova, E.; Rogach, A. L. Chiral carbon dots: synthesis, optical properties, and emerging applications. *Light Sci. Appl.* **2022**, *11* (1), 75.

[83] Xiao, Y.-H.; Ma, Z.-Z.; Yang, X.-X.; Li, D.-S.; Gu, Z.-G.; Zhang, J. Inducing Circularly Polarized Luminescence by Confined Synthesis of Ultrasmall Chiral Carbon Nanodot Arrays in Pyrene-Based MOF Thin Film. *ACS Nano* **2023**, *17* (19), 19136–19143.

[84] Zhang, Z.-C.; Jing, S.-M.; Ding, Q.-R.; Chang, L.-M.; Gu, Z.-G.; Zhang, J. Gel transformation fabrication of carbon nanodots incorporated chiral MOF film for circularly polarized afterglow. *Nano Res.* **2025**, *18* (6), 94907435.

[85] Li, Y.; Jiang, X.-X.; Xie, J.-X.; Lv, Y.-k. Recent Advances in the Application and Mechanism of Carbon Dots/Metal-Organic Frameworks Hybrids in Photocatalysis and the Detection of Environmental Pollutants. *Chem. Asian J.* **2022**, *17* (13), e202200283.

[86] Mahajan, M. R.; Nangare, S. N.; Patil, P. O. Nanosize design of carbon dots, graphene quantum dots, and metal–organic frameworks based sensors for detection of chlorpyrifos in food and water: A review. *Microchem. J.* **2023**, *193*, 109056.

[87] Ghahramani, Y.; Hajipour, N.; Tavakkol, O.; Gholami, M.; Yari Kalashgrani, M.; Neralla, V. R.; Chiang, W.-H.; Mousavi, S. M. Carbon Quantum Dot-Encapsulated Metal–Organic Framework Hybrids as Multifunctional Fluorescent Sensors for Oral Disease Biomarker Detection. *Chem. Rec.* **2025**, *25* (12), e202500146.

[88] Murugesan, A.; Li, H.; Shoaib, M. Recent Advances in Functionalized Carbon Quantum Dots Integrated with Metal–Organic Frameworks: Emerging Platforms for Sensing and Food Safety Applications. *Foods* **2025**, *14* (12), 2060.

[89] Zheng, W.-J.; Sun, Z.-N.; Wang, Y.-M.; Xiong, H.-M. Fluorescent carbon dots synthesized in solid phase and air for application in LEDs. *Nano Res.* **2024**, *17* (9), 8495–8503.

[90] Viravaux, C.; Mialane, P.; Dolbecq, A.; Ramsahye, N.; Mellot-Draznieks, C.; Serier-Brault, H.; Oms, O. Tunable ratiometric temperature sensors based on a Zn-MOF material incorporating luminescent polyoxometalates and carbon dots. *J. Mater. Chem. C* **2024**, *12* (38), 15535–15540.

[91] Han, S.; Chen, X.; Hu, Y.; Han, L. Solid-state N,P-doped carbon dots conquer aggregation-caused fluorescence quenching and couple with europium metal-organic frameworks toward white light-emitting diodes. *Dyes Pigments* **2021**, *187*, 109090.

[92] Dai, Y.; Hu, P.; Chu, T.; Niu, M.; Shi, H.; Li, H.; Wang, Z.; Guo, Y. Confinement of carbon dots into carboxymethyl cellulose matrice to prepare solid-state fluorescent films and couple with Eu-MOF toward white light-emitting diodes. *Int. J. Biol. Macromol.* **2025**, *296*, 139682.

[93] Wang, Z.; Yan, L.; Hao, Y.; Zheng, J.; Yang, Y.; Liu, X. Highly efficient and photothermally stable CDs@ZIF-8 for laser illumination. *Chinese Chem. Lett.* **2024**, *35* (10), 109430.

[94] Ma, Y.; Zhang, X.; Bai, J.; Huang, K.; Ren, L. Facile, controllable tune of blue shift or red shift of the fluorescence emission of solid-state carbon dots. *Chem. Eng. J.* **2019**, *374*, 787–792.

[95] Wu, S.; Yang, C.; Zhuang, J.; Chen, J.; Li, W.; Liu, Y.; Zheng, M.; Zhang, X.; Lei, B.; Guo, Y.; et al. Far-red emission carbon dot–metal organic frameworks composite for plant growth regulation application. *J. Mater. Chem. C* **2023**, *11* (39), 13370–13375.

[96] Xiao, L.; Cai, J.; Wang, Y.; Hu, J.; Dou, H.; Pan, D.; Geng, B.; Cheng, P.; Shen, L. Zr-Based Metal–Organic Framework Dual-Sensitized by Carbon Dot Sonosensitizers and MnO2−x Nanozymes for cGAS-STING Activation Enhanced Sonocatalytic-Immunotherapy. *Adv. Funct. Mater.* **2025**, *n/a* (n/a), e19998.

[97] Xie, Z.; Gao, Y.; Zuo, T.; Shen, C.; Jiang, H.; Xu, G.; Cen, Y.; Yang, J.; Hu, Q.; Li, R.; et al. Bifunctional Fe-CDs@MOF composite nanozyme based ratiometric fluorescent probe for the detection of xanthine in fish. *Talanta* **2025**, *293*, 128108.

[98] Su, Z.; Xu, H.; Zhang, Y.; Zhang, H.; Zhang, H.; Bao, Y.; Wu, X.; Yan, R.; Tan, G.; Wang, Z.; et al. A carbon dot-doped Cu-MOF-based smart nanoplatform for enhanced immune checkpoint blockade therapy and synergistic multimodal cancer therapy. *J. Mater. Chem. B* **2023**, *11* (19), 4211–4226.

[99] Nešić, M. D.; Popović, I. A.; Žakula, J.; Korićanac, L.; Filipović Tričković, J.; Valenta Šobot, A.; Jiménez, M. V.; Algarra, M.; Dučić, T.; Stepić, M. Synergistic Enhancement of Targeted Wound Healing by Near-Infrared Photodynamic Therapy and Silver Metal – Organic Frameworks Combined with S- or N-Doped Carbon Dots. *Pharmaceutics* **2024**, *16* (5), 671.

[100] Wu, X.; Tong, Z.; Liu, Y.; Yang, Y.; Li, Y.; Cheng, Y.; Yu, J.; Liu, N.; Jin, C.; Li, H. Cationic carbon dots: A novel class of mimetic enzymes. *Nano Res.* **2025**, *18* (4), 94907333.

[101] Tang, Y.; Xu, Q.; Zhang, X.; Zhu, R.; Zhao, N.; Wang, J. Expediting carbon dots synthesis by the active adaptive method with machine learning and applications in dental diagnosis and treatment. *Nano Res.* **2024**, *17* (11), 10109–10118.

[102] Yu, Z.; Deng, C.; Meng, L.; Wang, Y.; Li, C.; Liu, C.; Liu, Y.; Seidi, F.; Zhang, X.; Yong, Q.; et al. Closed-Loop Responsive Smart Bandages for Dynamic Monitoring and Self-Regulated Antibacterial Therapy in Wound Healing. *Adv. Funct. Mater.* **2025**, *n/a* (n/a), e20327.

[103] Dai, S.; Jiang, L.; Liu, L.; Su, Z.; Yao, L.; Yang, P.; Huang, N. MOF-encapsulated copper-doped carbon dots nanozymes with excellent biological activity promote diabetes wound healing. *Regen. Biomater.* **2024**, *11*, rbae119.

[104] Tang, C.; Liu, K.; Gao, X.; Kang, H.; Xie, W.; Chang, J.; Yin, L.; Kang, J. A metal-organic framework functionalized CaO2-based cascade nanoreactor induces synergistic cuproptosis/ferroptosis and Ca2+ overload-mediated mitochondrial damage for enhanced sono-chemodynamic immunotherapy. *Acta Biomater.* **2025**, *193*, 455–473.

[105] Shi, W.; Li, C.; Wang, N.; Lu, H.; Miao, G.; Cai, M.; Yang, J.; Zhang, Y.; Qu, Y.; Tang, Y.; et al. Fe-Doped Carbon Dots Control the Biodegradation Behaviors of Zr-Based Metal–Organic Framework for Tumor-Specific Chemotherapy and Ferroptosis Enhanced Sono-Chemodynamic Therapy. *Small* **2025**, *21* (32), 2502028.

[106] Bai, Y.; Zhao, J.; Zhang, L.; Wang, S.; Hua, J.; Zhao, S.; Liang, H. A

Smart Near-Infrared Carbon Dot-Metal Organic Framework Assemblies for Tumor Microenvironment-Activated Cancer Imaging and Chemodynamic-Photothermal Combined Therapy. *Adv. Healthcare Mater.* **2022**, *11* (12), 2102759.

[107] Lone, I. A.; Rohit, J. V. Carbon dots encapsulated metal-organic frameworks: An emerging optical sensors for monitoring of environmental pollutants. *Inorg. Chem. Commun.* **2025**, *180*, 114918.

[108] Qin, B.; Zhang, X.; Qiu, J.; Gahungu, G.; Yuan, H.; Zhang, J. Water-Robust Zinc–Organic Framework with Mixed Nodes and Its Handy Mixed-Matrix Membrane for Highly Effective Luminescent Detection of Fe3+, CrO42–, and Cr2O72– in Aqueous Solution. *Inorg. Chem.* **2021**, *60* (3), 1716–1725.

[109] Cai, J.; Hu, H.; Li, J.; Liao, J.; Gong, X. A color-changing carbon dots/hydrogel composite for human motion sensing and sweat pH detection. *Nano Res.* **2025**, *18* (2), 94907180.

[110] Lu, Y.; Dong, X.; Ji, G.; Wang, X.; Wang, T.; Tang, C.; Ola, O.; Duan, H.; Liu, Q.; Niu, Q. Anchor carbon dots inside NH2-MIL-88B via ship-in-a-bottle strategy for dual signal enhancement in colorimetric-fluorescent sensors. *Sensors Actuat. B-Chem.* **2025**, *424*, 136877.

[111] Qin, B.; Zhang, X.; Dang, J.; Yue, D.; Zhang, B.; Li, W.; Gahungu, G.; Wang, Z.; Zhang, J. A 2-fold interpenetrated zinc–organic framework with Lewis basic triazole sites: luminescence sensing of Fe3+ and Cr2O72−, and warm white-light emission by encapsulated Ln3+ ions. *CrystEngComm* **2022**, *24* (40), 7058–7065.

[112] Wang, Y.; Wei, X.; Su, Y.; Xu, R.; Song, D.; Ding, L.; Chen, Y. Highly sensitive fluoroprobe for detecting Sudan dyes in paprika utilizing carbon dot-embedded zeolitic imidazolate framework-8. *Food Chem.* **2024**, *438*, 137975.

[113] Wang, M.; Zhou, M.; Wang, M.; Du, J.; Liu, C.; Wang, Y.; Xia, Z. Fabrication of a bifunctional fluorescent chiral composite based on magnetic Fe3O4/chiral carbon dots@hierarchical porous metal-organic framework. *Talanta* **2024**, *266*, 125113.

[114] Yan, D.; Yuan, F.; Chen, Z.; Zhang, J.; Song, S. Eu-doped carbon dots-MOF based turn-on fluorescent probe for trace Hg2+ and Pb2+ and construction of the simultaneous detection model. *Chem. Eng. J.* **2024**, *499*, 156102.

[115] Hui, Y.; Wei, Y.; Guo, H.; Wang, M.; Peng, L.; Ren, B.; Ma, Y.; Yang, W. An artificial neural network model based on CDs@MOF/COF composites for the ultra-sensitive fluorescence detection of glyphosate. *Food Chem.* **2025**, *492*, 145361.

[116] Wang, Y.; Wang, K.; Wang, M.; Shan, R.; Li, X.; Zhang, H. Novel ratiometric fluorescence sensor for organophosphorus pesticides via carbon dots supported zirconium-based metal organic frameworks. *Food Control* **2025**, *171*, 111095.

[117] Yan, F.; Wang, X.; Wang, Y.; Yi, C.; Xu, M.; Xu, J. Sensing performance and mechanism of carbon dots encapsulated into metal–organic frameworks. *Microchim. Acta* **2022**, *189* (10), 379.

[118] Luo, X.; Huang, G.; Li, Y.; Guo, J.; Chen, X.; Tan, Y.; Tang, W.; Li, Z. Dual-modes of ratiometric fluorescent and smartphone-integrated colorimetric detection of glyphosate by carbon dots encapsulated porphyrin metal–organic frameworks. *Appl. Surf. Sci.* **2022**, *602*, 154368.

[119] Olorunyomi, J. F.; White, J. F.; Gengenbach, T. R.; Caruso, R. A.; Doherty, C. M. Fabrication of a Reusable Carbon Dot/Gold Nanoparticle/Metal–Organic Framework Film for Fluorescence Detection of Lead Ions in Water. *ACS Appl. Mater. Interfaces* **2022**, *14* (31), 35755–35768.

[120] Wan, H.; Wang, X.; Lin, C.; Wang, L.; Liu, L.; Song, Y. Carbon dot@metal-organic frameworks with aggregation-induced emission for visual detection of ascorbic acid. *Spectrochim. Acta A* **2026**, *348*, 127074.

[121] Ma, X.; Ou, Q.; Yuan, J.; Yang, J.; Xu, S.; Zhang, X. Multifunctional Fe-doped carbon dots and metal-organic frameworks nanoreactor for cascade degradation and detection of organophosphorus pesticides. *Chem. Eng. J.* **2023**, *464*, 142480.

[122] Fang, J.; Li, M.; Cao, D.; Zhang, J.; Wang, H.; Cao, W.; Wei, Q. Restricted-Enhanced Electrochemiluminescence biosensor of low excitation potential carbon quantum dots driven by magnetic Metal-Organic frameworks for sensitive immunoassay of neuron specific enolase. *Chem. Eng. J.* **2024**, *498*, 155660.

[123] Li, C.; Hang, T.; Jin, Y. Atomically Fe-anchored MOF-on-MOF nanozyme with differential signal amplification for ultrasensitive cathodic electrochemiluminescence immunoassay. *Exploration* **2023**, *3* (4), 20220151.

[124] Wang, H.; Liu, P.; Peng, J.; Yu, H.; Wang, L. Poly(3,4-ethylenedioxythiophene):poly(styrene sulfonate) modified metal-organic frameworks boosting carbon dots electrochemiluminescence emission for sensitive miRNA detection. *Biosens. Bioelectron.* **2024**, *249*, 116015.

[125] Liu, J.; Wang, Y.; He, M.; Chen, X.; Zhou, C.; Li, J. Self-cascade catalytic system constructed using carbon dots and Au nanoparticles co-assembled on MIL-53(Fe)-NH2 as a three-in-one fluorescent nanozyme for multimodal detection of glucose and maltose in food. *Food Chem.* **2025**, *468*, 142485.

[126] Liang, M.; Gao, Y.; Sun, X.; Kong, R.-M.; Xia, L.; Qu, F. Metal-organic framework-based ratiometric point-of-care testing for quantitative visual detection of nitrite. *J. Hazard. Mater.* **2024**, *469*, 134021.

[127] Pathan, S.; Raveendran, J.; Memon, M.; Chavda, V.; Niyas, K.; Bayry, J.; Rasheed, P. A. Upcycling of electronic waste into a Cu-based metal–organic framework: From cell phone to a disposable electrochemical bilirubin sensor. *Chem. Eng. J.* **2025**, *511*, 162217.

[128] Pan, W.; Zhu, Z.-H.; Zhao, Y.-S.; Jie, L.; Zhang, Z.-G.; Li, G.-X.; Yu, T.; Han, Z.-Z.; Long, Y.-Z.; Yu, G.-F. Chitosan/PEO@Eu-MOF nanofiber membrane-based test strip for visual detection of tetracycline with smartphone-assisted analysis. *Chem. Eng. J.* **2025**, *520*, 165936.

[129] Chen, J.; Wang, Y.; Shen, R.; Li, W.; Gao, S.; Xiao, Z.; Lv, Q.; Song, X.; Xu, J.; Xu, G.; et al. Accurately Tunable AuNC-ZIF Content Architecture Based on Coordination-Dissociation Mechanism Enables Highly Brightness Dual-Site Fluorescent Biosensor. *Adv. Sci.* **2025**, *12* (4), 2408400.

[130] Liu, M.; Liu, Y.; Xiao, J.; Ren, Y.; Gao, X. Colorimetric-ratiometric fluorescence sensors dual-mode detection of ofloxacin based on Fe-Ni bimetallic metal-organic frameworks and carbon dots. *Food Control* **2025**, *169*, 110989.

[131] Zhang, J.; Wang, T.; Du, Y.; Wu, Y.; Jiang, X.; Zou, H.; Zhang, Z. Smartphone-assisted ratiometric fluorescence sensor based on NS-codoped carbon dots/Au nanoclusters for rapid detection of Hg2+. *Microchem. J.* **2024**, *199*, 110201.

[132] Zheng, X. T.; Leoi, M. W. N.; Yu, Y.; Tan, S. C. L.; Nadzri, N.; Goh, W. P.; Jiang, C.; Ni, X. P.; Wang, P.; Zhao, M.; et al. Co-Encapsulating Enzymes and Carbon Dots in Metal–Organic Frameworks for Highly Stable and Sensitive Touch-Based Sweat Sensors. *Adv. Funct. Mater.* **2024**, *34* (10), 2310121.

[133] Lin, X.; Cao, Z.; Zeng, S.; Zhu, H.; Zhai, K.; Yin, B.; Zhang, C.; Peng, T.; Cheng, T.; Zhang, B. Portable dual-mode microfluidic sensor for rapid and sensitive detection of DPA on chip. *Adv. Compos. Hybrid. Mater.* **2025**, *8* (3), 240.

[134] Poojary, M. M.; Lund, M. N. Chemical Stability of Proteins in Foods: Oxidation and the Maillard Reaction. *Annu. Rev. Food Sci. Technol.* **2022**, *13*, 35–58.

[135] Alizadeh Sani, M.; Jahed-Khaniki, G.; Shariatifar, N.; Khezerlou, A.; Abedini, A.; Rezvani-Ghalhari, M.; Hassani, S.; Tavassoli, M.; McClements, D. J. Metal Organic Frameworks (MOFs) as Advanced Functional Materials for Food Applications. *ACS Food Sci. Technol.* **2024**, *4* (10), 2272–2300.

[136] Ananthi, P.; V, N. R.; K, H.; A, P.; Pius, A. Fluorescence Resonance Energy Transfer in Gelatin-Based MOF/N-CDs Films for Superior Photodynamic Antibacterial Packaging Materials. *ACS Sustainable Chem. Eng.* **2025**, *13* (8), 3052–3065.

[137] Sultana, A.; Kathuria, A.; Gaikwad, K. K. Metal–organic frameworks for active food packaging. A review. *Environ. Chem. Lett.* **2022**, *20* (2), 1479–1495.

[138] Hong, S. J.; Riahi, Z.; Shin, G. H.; Kim, J. T. Poly(vinyl alcohol)-based multifunctional smart packaging films with carbon dots-loaded metal-

organic frameworks for freshness indicator and shelf-life extension of shrimp. *Prog. Org. Coat.* **2025**, *198*, 108899.
[139] Ti, Y.; Qin, Z.; Guo, X.; Wu, Z.; Jiang, Q.; Dong, B.; Fawole, O. A.; Wu, D.; Chen, S.; Li, X.; et al. Fabrication of Dual Photodynamic Enhanced Antimicrobial CDs@ZIF-8/Polycaprolactone/Ethyl Cellulose Nanofibrous Films for Fruit Preservation. *Adv. Sci.* **2025**, *12* (35), e03567.
[140] Riahi, Z.; Khan, A.; Rhim, J.-W.; Shin, G. H.; Kim, J. T. Synergistic effect of iron-based metal-organic framework hybridized with carbon quantum dots in agar/gelatin films for fruit preservation. *Food Packag. Shelf Life* **2024**, *45*, 101330.